GAC MEDALLIST SERIES

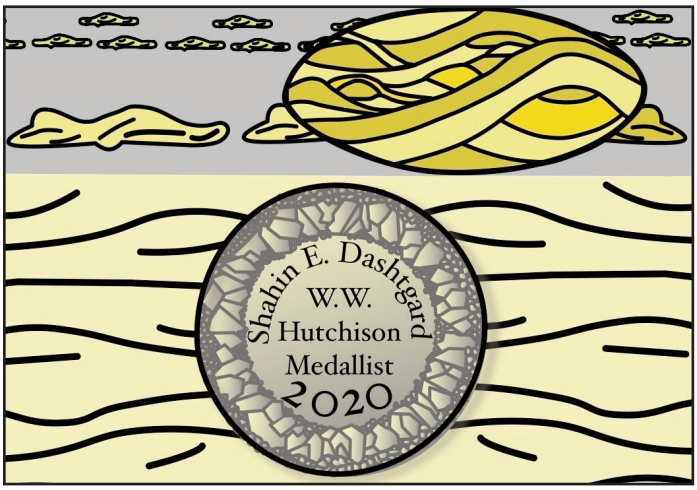

Hutchison Medallist 1. Wave-Dominated to Tide-Dominated Coastal Systems: A Unifying Model for Tidal Shorefaces and Refinement of the Coastal-Environments Classification Scheme

Shahin E. Dashtgard[1], Romain Vaucher[1], Byongcheon Yang[2], and Robert W. Dalrymple[3]

[1]Applied Research in Ichnology and Sedimentology (ARISE) Group
Department of Earth Sciences, Simon Fraser University
Burnaby, British Columbia, V5A 1S6, Canada
E-mail: sdashtga@sfu.ca

[2]Korea National Oil Corporation
305 Jongga-ro, Jung-gu, Ulsan, 44538, South Korea

[3]Department of Geological Sciences and Geological Engineering
Queen's University, Kingston, Ontario, K7L 3N6, Canada

SUMMARY

Coastal depositional systems are normally classified based on the relative input of wave, tide, and river processes. While wave- through to river-dominated environments are well characterized, environments along the wave-to-tide continuum are relatively poorly understood and this limits the reliability and utility of coastal classification schemes. Two tidal shoreface models, open-coast tidal flats (OCTF) and tidally modulated shorefaces (TMS), have been introduced for mixed wave-tide coastal settings. Following nearly two decades of research on tidal shorefaces, a number of significant insights have been derived, and these data are used here to develop a unified model for such systems. First, OCTFs are components of larger depositional environments, and in multiple published examples, OCTFs overlie offshore to lower shoreface successions that are similar to TMS. Consequently, we combine OCTFs and TMSs into a single tidal shoreface model where TMS (as originally described) and TMS-OCTF successions are considered as variants along the wave-tide continuum. Second, tidal shoreface successions are preferentially preserved in low- to moderate- wave energy environments and in progradational to aggradational systems. It is probably difficult to distinguish tidal shorefaces from their storm-dominated counterparts. Third, tidal shorefaces, including both TMSs and OCTFs, should exhibit tidally modulated storm deposits, reflecting variation in storm-wave energy at the sea floor resulting from the rising and falling tide. They may also exhibit interbedding of tidally generated structures (e.g. double mud drapes or bidirectional current ripples), deposited under fairweather conditions, and storm deposits (e.g. hummocky cross-stratification) through the lower shoreface and possibly into the upper shoreface.

The development of the tidal shoreface model sheds light on the limitations of the presently accepted wave-tide-river classification scheme of coastal environments and a revised scheme is presented. In particular, tidal flats are components of larger depositional systems and can be identified in the rock record only in settings where intertidal and supratidal deposits are preserved; consequently, they should not represent the tide-dominated end-member of coastal systems. Instead, we suggest that tide-dominated embayments should occupy this apex. Tide-dominated embayments exhibit limited wave and river influence and include a wide range of geomorphological features typically associated with tidal processes, including tidal channels, bars and flats.

RÉSUMÉ

Les systèmes de dépôts côtiers sont normalement classés en fonction de l'apport relatif des processus liés à la houle, aux marées et aux rivières. Si les environnements dominés par la houle et les rivières sont bien caractérisés, les environnements le long du continuum houle-marée sont relativement mal compris, ce qui limite la fiabilité et l'utilité des systèmes de classifi-

Geoscience Canada, v. 48, https://doi.org/10.12789/geocanj.2021.48.171 pages 5–22 © 2021 GAC/AGC®

cation des côtes. Deux modèles d'avant-plages tidales, les estrans ouverts (*open-coast tidal flats*; OCTF) et les avant-plages modulées par la marée (*tidally modulated shoreface*; TMS), ont été introduits pour les milieux côtiers mixtes, houle-marée. Suite à près de deux décennies de recherche sur les avant-plages tidales, un certain nombre d'informations importantes ont été obtenues et ces données sont utilisées ici pour développer un modèle unifié pour ces systèmes. Tout d'abord, les OCTF sont les composants de systèmes de dépôt plus vastes et, dans de nombreux exemples publiés, les OCTF recouvrent des successions sédimentaires allant du large à l'avant-plage inférieure, similaires à celle des TMS. Par conséquent, nous combinons les OCTF et les TMS en un seul modèle d'avant-plage tidale où les TMS (tel que décrit à l'origine) et les successions TMS-OCTF sont considérés comme des variantes le long du continuum houle-marée. Deuxièmement, les successions d'avant-plages tidales sont préférentiellement préservées dans des environnements ayant une houle faible à modérée et dans des systèmes progradant et aggradant. Il est probablement difficile de distinguer les avant-plages tidales de leurs homologues dominés par les tempêtes. Troisièmement, les avant-plages tidales, incluant à la fois les TMS et les OCTF devraient présenter des dépôts de tempête modulés par la marée, reflétant ainsi la variation de l'énergie des vagues de tempête sur le fond marin liée à la marée montante et descendante. Les avant-plages tidales peuvent également présenter une interstratification de structures générées par la marée (par exemple, des doubles drapages argileux ou des rides de courants bidirectionnelles) déposées pendant des conditions de beau temps, et des dépôts de tempête (par exemple, des stratifications en mamelons) au niveau de l'avant-plage inférieure et éventuellement de l'avant-plage supérieure.

Le développement du modèle d'avant-plage tidale met en lumière les limites de la classification tripartite (houle-marée-rivière) des environnements côtiers actuellement acceptée et une classification révisée est présentée. En particulier, les OCTF et les estrans sont des composantes de systèmes de dépôt plus importants et ne peuvent être identifiés que dans le registre sédimentaire dans les milieux où les dépôts intertidaux et supratidaux sont préservés; par conséquent, ils ne devraient pas représenter le membre extrême des systèmes côtiers dominé par la marée. Nous suggérons plutôt que les baies dominées par la marée occupent cette place. Les baies dominées par les marées présentent une influence limitée des vagues et des rivières et comprennent un large éventail de caractéristiques géomorphologiques généralement associées aux processus de marée, notamment des chenaux, des barres et des platiers tidaux.

1. INTRODUCTION

Coastal systems and their associated deposits are extremely diverse, yet sedimentological models promote the notion that coastal deposits can be identified as wave-, tide-, or river-dominated (or any combination of the three) on the basis of their sedimentary features. The tripartite process-based subdivision of coastal systems was first introduced by Galloway (1975) for deltas and later expanded to include all coastal to shallow marine systems (Fig. 1A; Boyd et al. 1992; Ainsworth et al. 2011). These classification schemes proved useful for distinguishing and classifying large scale variations in the geomorphology of coastal environments as a function of relative energy input, but significant issues remained within classification schemes, especially along the wave- to tide- continuum. Wave- and tide-dominated settings are distinctive in terms of their physical processes and geomorphology, and this results in the two end-member environments, beach-shorefaces (wave-dominated) and tidal flats (tide-dominated), exhibiting distinctive facies and grain-size distributions (e.g. Weimer et al. 1982; Dalrymple 2010; Plint 2010; Dashtgard et al. 2012; Pemberton et al. 2012). A range of mixed wave-tide settings (i.e. tidal shorefaces) occur between the wave-dominated and tide-dominated end members, and sedimentological signatures of both tide- and wave-processes are manifested in these mixed influence systems (Fig. 1B; Yang et al. 2005; Dashtgard et al. 2009).

Herein, we consider depositional models that have been proposed for coastal to shallow marine systems along the wave-tide continuum. We compare and contrast two closely related tidal-shoreface variants, open-coast tidal flats (OCTF) and tidally modulated shorefaces (TMS), both of which have been proposed for mixed wave-tide coastlines. Over the past 10 years, deposits interpreted as either OCTF or TMS have been described from the sedimentary record and this literature is summarized and compared to the original models (Table 1; Basilici et al. 2012; Smosna and Bruner 2016; Wei et al. 2016; Vaucher et al. 2017, 2020; Bádenas et al. 2018; MacNaughton et al. 2019; Angus et al. 2020; Kalifi et al. 2020; Sleveland et al. 2020). We then propose a unified model for tidal shorefaces taking into account the multiple variants described so far. Second, we propose a revision to the classification scheme for coastal environments that incorporates our findings and other insights on wave-, tide-, and mixed wave-tide coastal systems. The revised classification scheme better encapsulates the range of coastal settings that occur along the wave-tide continuum and how they relate to other environments with changes in relative energy input from waves, tides and rivers.

1.1 End Member Systems – Beaches and Shorefaces

One of the earliest beach-shoreface models was developed for gravel beaches and showed the distribution of clasts across the beach as a function on grain shape and size (Bluck 1967). Sand-dominated beach-shoreface systems received significantly more attention, and it has been demonstrated repeatedly that the distribution of sedimentary structures in these wave-dominated settings is controlled by a predictable distribution of oscillatory processes and wave-induced currents in increasingly shallow water up through the shoreface and onto the beach face (Fig. 2; e.g. Psuty 1967; Galvin 1968; Clifton 1969; Clifton et al. 1971; Davies et al. 1971; Kumar and Sanders 1976). Storm influence on shorefaces was also noted very early in the study of beach-shoreface systems (Bluck 1967; Hayes 1967; Clifton et al. 1971) indicating that storm influence is a ubiquitous contribution to shoreface development. Based on the relative impact of storm-wave versus fairweather wave processes on deposition, three end-member shoreface successions were

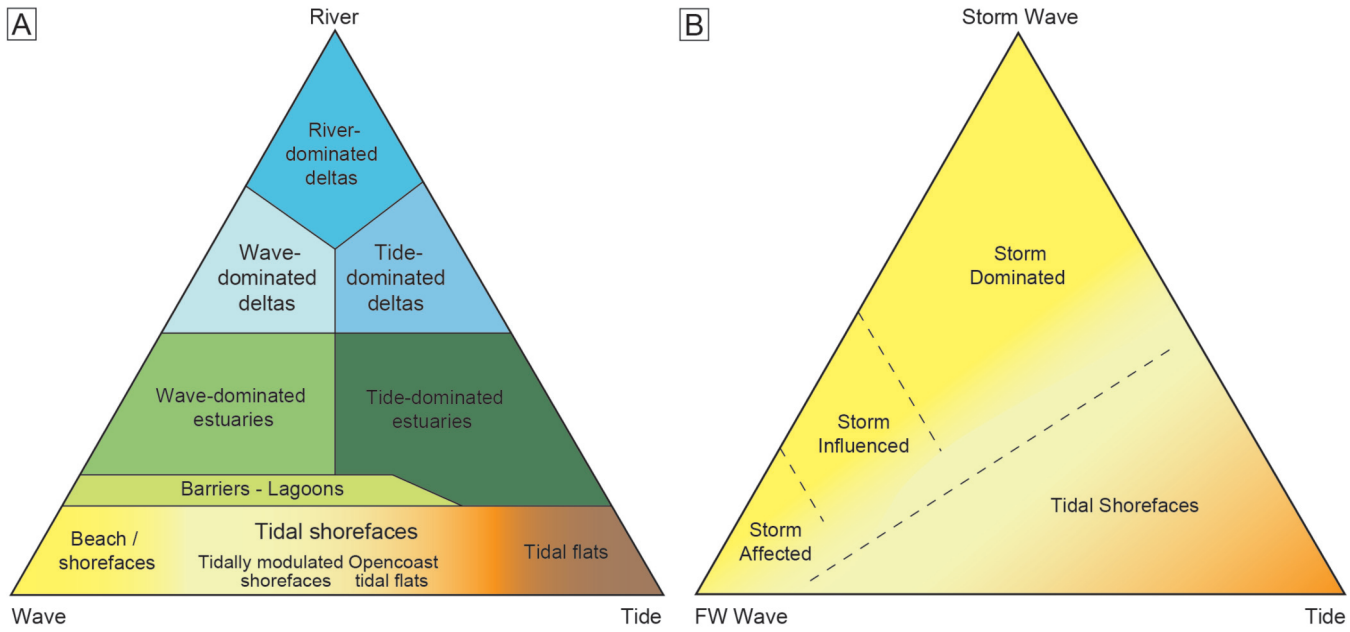

Figure 1. A) Ternary diagram showing the relative distribution of coastal to shallow-marine systems relative to the degree of wave-, tide-, and river input/energy (modified after Boyd et al. 1992; Yang et al. 2005). B) Ternary diagram for mixed wave-tide systems wherein waves are divided between fairweather (FW) and storm waves. Note the dominance of storm-wave processes in determining the character of the preserved deposit (modified after Dashtgard et al. 2012).

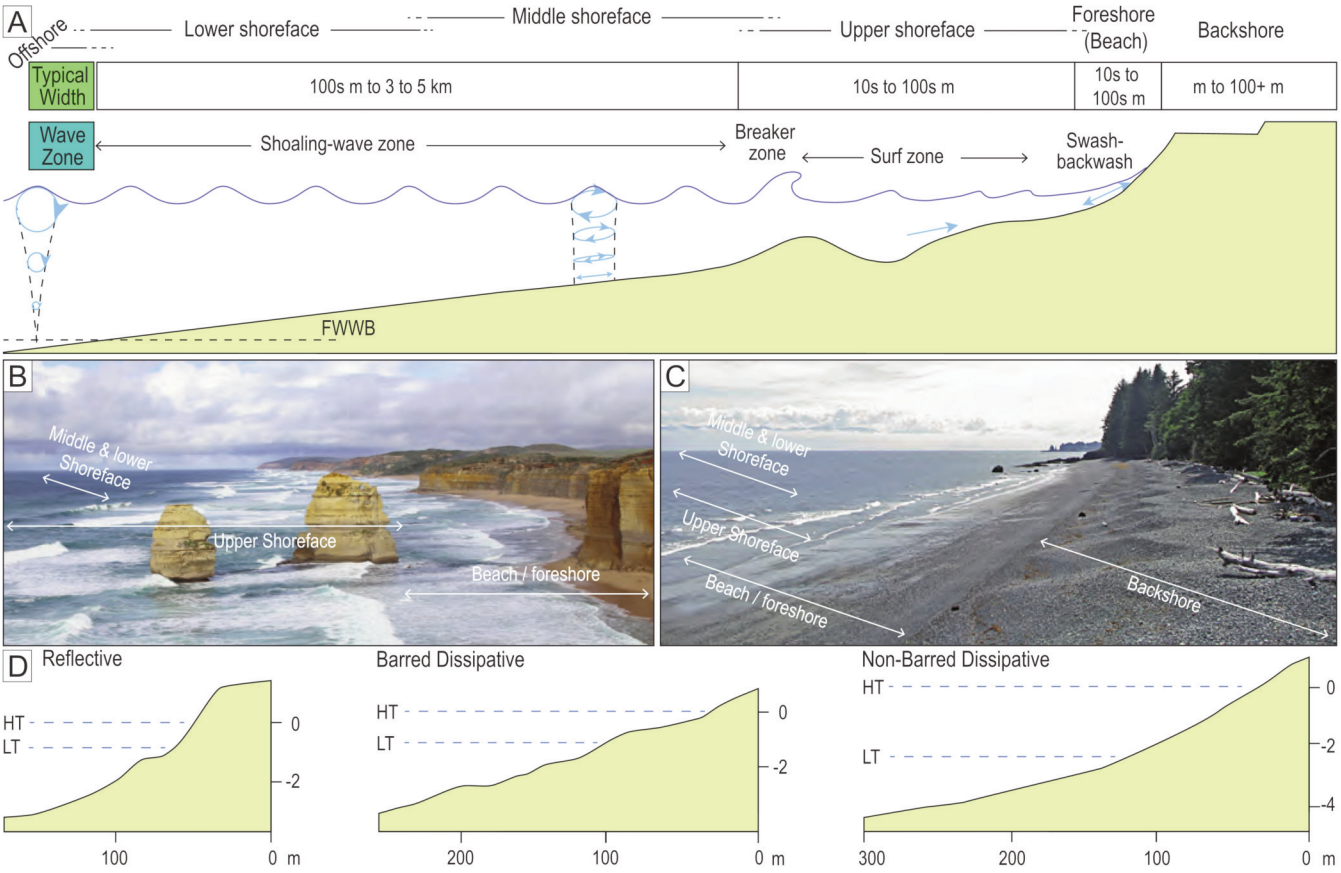

Figure 2. Conceptual models for wave-dominated beach-shorefaces. A) An idealized profile of a beach-shoreface system showing the distribution of wave processes and shoreface subenvironments from offshore to the backshore, and the general range for the shore-normal width of those zones. B) Photo of the shoreface and beach at the Twelve Apostles (Victoria, Australia) with wave zones indicated. C) Photo of Sandcut Beach (south coast of Vancouver Island, Canada) with wave zones indicated. D) Three morphological profiles proposed by Masselink and Short (1993) for shorefaces with limited tide-influence relative to wave influence. Acronyms: low tide (LT), high tide (HT), fairweather wave base (FWWB).

https://doi.org/10.12789/geocanj.2021.48.171

Table 1 – Summary of geological units interpreted as tidal shorefaces. General context and recognition criteria used by the original authors are listed.

Interpretation	Geological Unit	Age	Location	Context of Deposition	Recognition Criteria	References
Wave-dominated open-coast tidal flat	Lagarto and Palmares formations	Cambrian–Ordovician	Brazil	Foreland basin	(i) Wave processes are indicated by wave ripples and HCS. (ii) Tidal processes are interpreted from cross-stratification (tidal bundles); climbing ripples that alternate repeatedly with mud drape lenses; stacked ripples; wavy lamination and wave ripples in anisotropic HCS beds; flaser, wavy and lenticular bedding; bidirectional ripples alternating with mudstone beds; and, herringbone cross-bedding.	Basilici et al. 2012
Tide-dominated beach	Cabos Formation	Middle Cambrian – Early Ordovician	Spain	Post-rift	(i) Interpreted beach deposits comprise small 2-D dunes composed of fine-grained sand (ridge-and-runnel system). Dunes form via wave processes and are interpreted to have both accreted upward and migrated landward during rising tide, and then subsequently reworked by ebb currents and surface runoff during periods of emergence. (ii) Tidal reworking was interpreted from herringbone cross-bedding, discontinuity surfaces, and superimposed bed forms. Associated structures formed near low tide include interference ripples, double-crested ripples, flat-topped ripples, current ripples with muddy troughs, and mudstone partings. (iii) Rhythmically interbedded mud and sand with sparse bioturbation is interpreted to record accumulation in the subtidal nearshore. Tides and waves formed uni- and bidirectional current ripples, oscillatory wave ripples, combined-flow ripples, erosional sand mounds, rhythmic bedding, and heterolithic bedding.	Smosna and Bruner 2016
Storm-dominated, tide-influenced delta front	Rannoch Formation	Middle Jurassic Aalenian	Northern North Sea	Pre-rift	Two facies are frequently interbedded and form "storm-tide couplets". The two facies include (i) thin mud drapes and double mud drapes that comprise up to 15% of the entire thickness and are interpreted as tidal deposits formed during fairweather conditions. These beds are preserved between (ii) unburrowed, well-sorted sandy beds reflecting storm events that lack a capping bioturbated mudstone interval.	Wei et al. 2016
Tidally modulated ridge-and-runnel upper shoreface	Fezouata Shale and Zini Formation	Early Ordovician Tremadocian - Floian	Morocco	Post-rift, passive margin	(i) Symmetrical and slightly asymmetrical oscillatory related sedimentary structures of various wavelengths interbedded with dominantly low-angle or plane-parallel stratification suggest tide modulation of wave processes in the upper shoreface-foreshore. (ii) Combined-flow ripples that show evidence of both aggradation and migration alternate with purely aggrading wave ripples/HCS. This is interpreted as recording tide-modulated storm deposits. (iii) Ubiquitous stacking of oscillatory-induced structures of shorter-to-longer wavelengths reflects continuous tide modulation of the wave action on the seafloor.	Vaucher et al. 2017, 2018a

*Acronyms: hummocky cross-stratification (HCS); swaley cross-stratification (SCS)

Table 1 – *(Cont.)* Summary of geological units interpreted as tidal shorefaces. General context and recognition criteria used by the original authors are listed.

Interpretation	Geological Unit	Age	Location	Context of Deposition	Recognition Criteria	References
Mixed (clastic and carbonate), wave (storm)-dominated open coast tidal flat	Aguilar del Alfambra Formation	Late Jurassic Tithonian - Berriasian	Spain	Syn-rift	(i) Thinning and finning upward, poorly bioturbated heterolithic interval displaying HCS, and current, wave and combined-flow ripples reflect together open-coast tidal flat deposits. (ii) Several beds showing a vertical evolution form current to combined-flow ripples to HCS are observed within (i) and possibly point a tide-modulation of storm waves across the intertidal zone.	Bádenas et al. 2018
Wave-dominated tidal-flat	Elk Mound Group	Late Cambrian Miaolingian - Furongian	U.S.A.	Epeiric sea	Sedimentary structures reflecting storm wave deposition (parallel-lamination, cross-bedding, but no hummocky cross-stratification) and fairweather deposition (oscillation ripples) occur concomitantly. Indicators of fluctuations in water depth (washouts, flat-topped ripples and stranded medusoids) and subaerial exposure (desiccation cracks, raindrop imprints and adhesion marks) are present.	MacNaughton et al. 2019
Tidally modulated, barred shoreface	Weald Basin	Late Jurassic Kimmeridgian - Tithonian	England / France	Extensional basin	(i) Pervasive interstratification of wave-formed sedimentary structures that are interpreted as forming at different depths occur throughout and reflect repeated variations in water depth induced by tides. This is interpreted as tide modulation of wave processes (ii) Upper shoreface and foreshore deposits are abnormally thick. (iii) Trace fossils typically attributed to either the *Skolithos* or *Cruziana* Ichnofacies co-occur within lower shoreface deposits.	Angus et al. 2020
Open-coast intertidal	Upper Marine Molasse	Miocene Upper Aquitanian - Langhian	France	Foreland basin	(i) Plane-parallel lamination vertical evolving into SCS/HCS within the same sandstone bed suggest tide modulation of wave processes. (ii) Combined-flow ripples frequently display oblique foresets with downcutting in their bottomsets pointing out an increase of the tidal flow while the structures developed (see text for explanation).	Kalifi et al. 2020
Storm-Influenced subtidal flat	Upper Mulichinco Formation	Early Cretaceous Valanginian	Argentina	Post-rift / back-arc	Interbedding of (i) weakly bioturbated, well-sorted sandstones displaying HCS, SCS, low-angle and trough cross-stratification with isolated *Thalassinoides*, *Gyrochorte*, and *Ophiomorpha*. and either (ii) trough cross-stratified muddy sandstone with reactivation surfaces, herringbone, current and combined-flow ripples, bundled symmetric ripples, climbing ripples, lenticular, wavy, and flaser bedding, or (iii) extensively bioturbated sandstone beds reflects storm events (i) in subtidal environments (ii and iii).	Sleveland et al. 2020
Wave-dominated tide-modulated foreshore	Angosto del Moreno Formation	Late Cambrian Furongian	Argentina	Extensional basin	Interbedding of (i) low-angle planar-laminated, unbioturbated fine- to medium-grained sandstone (i.e. swash cross-stratification) and (ii) sandstone having symmetrical and asymmetrical ripples and rare trace fossils is interpreted as reflecting deposition in a wave-dominated, tidally modulated foreshore, where planar bedding (i) is formed by swash processes (at low tide) and alternates with combined-flow to oscillatory processes stemming from wave and tide processes (at high tide; (ii)).	Vaucher et al. 2020

*Acronyms: hummocky cross-stratification (HCS); swaley cross-stratification (SCS)

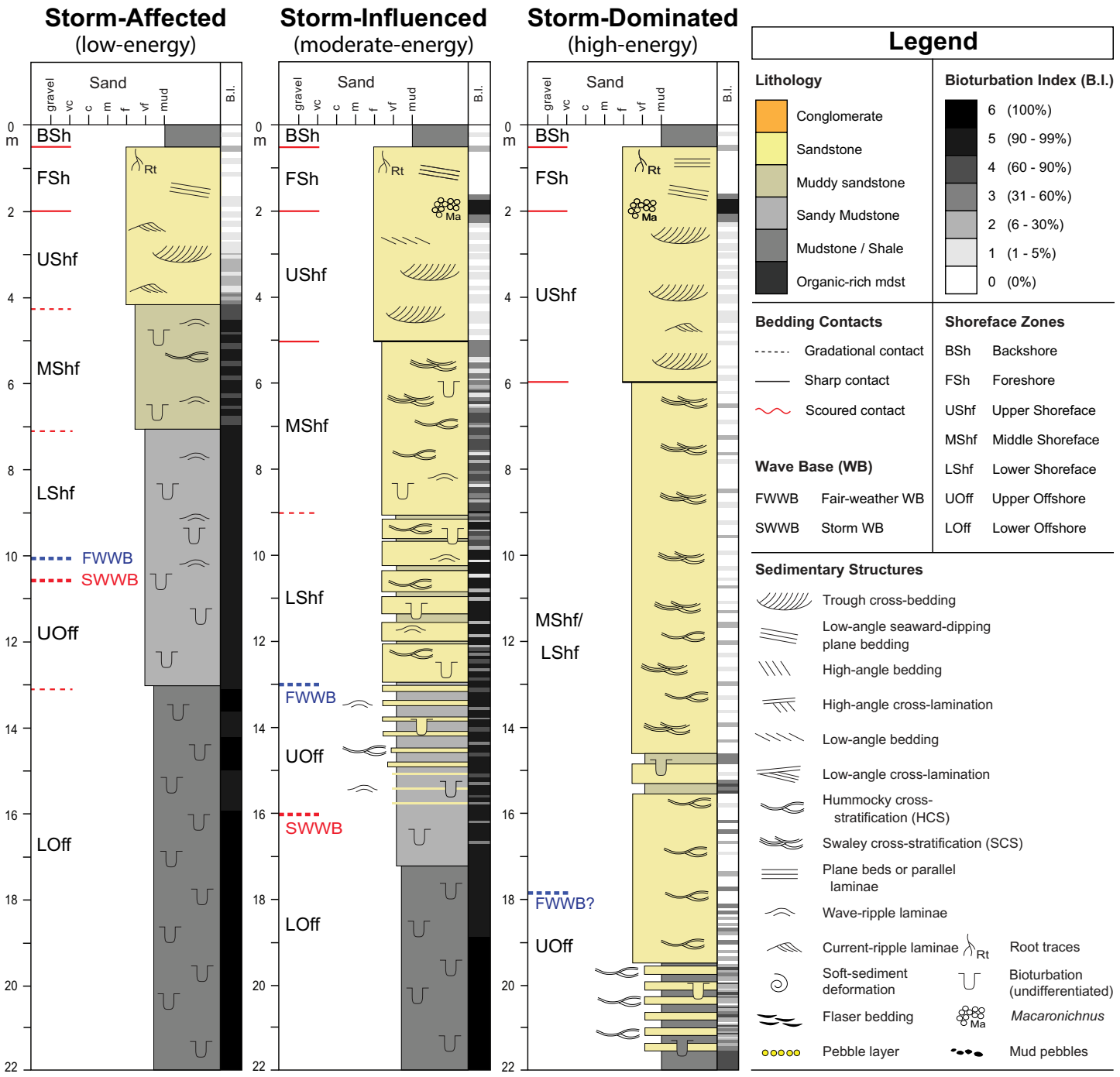

Figure 3. Conceptual models for three archetypes of wave-dominated shorefaces that show increasing storm influence from storm-affected to storm-dominated. The revised names of each shoreface archetype proposed herein is shown in brackets below the names for each succession. Note the increase in thickness of the upper shoreface and foreshore, and the amalgamation of HCS/SCS with increasing storm influence in high-energy settings (modified after Dashtgard et al. 2012).

proposed, including (in order of increasing storm-wave influence): storm-affected, storm-influenced, and storm-dominated (Figs. 1B and 3; Clifton 2006; Dashtgard et al. 2012). This nomenclature is discussed further in Section 5. In all progradational, wave-dominated shoreface variants, grain size coarsens upward from offshore to the surf zone (Fig. 3), and this reflects the increase in effective wave energy in increasingly shallow water up the shoreface (Fig. 2).

1.2 End Member Systems – Tidal Flats

At the other end of the spectrum of wave-tide systems are tidal flats (Fig. 1A), which have been described extensively in the literature. Models for tidal flats are largely derived from modern settings due to the ease of accessing these environments during low tide (e.g. Häntzschel 1939; Van Straaten 1961; Kellerhals and Murray 1969; Reineck 1975; Swinbanks and Murray 1981; Weimer et al. 1982; Dalrymple 1992, 2010).

Tidal flats commonly occur in protected settings with very low depositional slopes (Van Straaten and Kuenen 1957; Van Straaten 1961; Reineck 1975; Ainsworth et al. 2015) and/or in restricted waterways and embayments, including estuarine and back-barrier systems (i.e. areas that are sometimes referred to as "inshore" settings; Dashtgard 2011b; Flemming 2012). They develop as a result of low levels of wave action, due either to sheltering or attenuation by frictional retardation of wave-orbital motion and wave-forced currents across the flats, accompanied by tidal-current amplification and tidally induced water-level fluctuations. Deposition is controlled mainly by the settling and scour lags, processes that control the landward movement of fine-grained sediment in a tidal environment (Van Straaten and Kuenen 1958; Dalrymple and Choi 2003; Pritchard and Hogg 2003), and grain size varies as a function of both sediment input and river-, wave-, and tide-influence. Progradational tidal flats typically become finer toward the high-tide shoreline and are manifested in the rock record as fining-upwards successions. This reflects the onshore decrease in depositional energy which results in both an onshore decrease in grain size and a landward increase then decrease in the intensity of bioturbation from the low to high intertidal zone (Fig. 4). In inshore settings, tidal flats typically overlie channelized facies; however, tidal flats also commonly overlie other depositional systems (e.g. shorefaces and delta fronts; Weimer et al. 1982; Dalrymple 2010; Dashtgard 2011a, b). This association of tidal flats with other shallow-marine subenvironments reflects the fact that tidal flats are developed in the shallowest water positions (equivalent to the upper shoreface and beach) of coastal depositional environments.

2. MIXED WAVE-TIDE SYSTEMS

The expression of tidal processes in beach-shoreface systems was largely overlooked in early models with the exception of recognizing the intertidal zone (the beach/foreshore zone; Fig. 2). Tidal influence on the geomorphology of beach-shoreface systems was explored in the 1980s and 1990s (Fig. 5; Short 1984, 1991, 1999; Masselink and Short 1993; Masselink and Hegge 1995), but sedimentological models that incorporated expressions of tidal processes in the preserved character and architecture of shorefaces did not occur until the mid- to late-2000s with competing and, in some cases, complementary models for open-coast tidal flats (OCTF; Yang et al. 2005, 2006, 2008b), tidally modulated shorefaces (TMS; Dashtgard et al. 2009; Dashtgard et al. 2012; Pemberton et al. 2012; Vaucher et al. 2018a), micro-meso tidal shorefaces (Vakarelov et al. 2012), and tide-influenced shorefaces (Frey and Dashtgard 2011; Dashtgard et al. 2012). With the exception of the micro-meso tidal shoreface model (Vakarelov et al. 2012), all models were developed in modern depositional settings.

Herein, "tidal shorefaces" encompass depositional environments along the wave-tide spectrum wherein both wave- and tidal-processes operate and are recognizable in the sedimentary record (Figs. 5–7). The earliest model for one element of tidal shorefaces, the OCTF, was developed from a very fine- to fine-grained sandy tidal flat (the Baeksu tidal flat) along the west coast of Korea (Fig. 5). This system experiences meso- to macro-tidal conditions (mean tidal range: 3.9 m; maximum range: 6.8 m), with small waves during the summer monsoon season, and large waves during the winter and infrequent tropical cyclones during the summer and fall. The stark contrast in wave energy between the summer and winter is manifested in the sediment. Indeed, the flats exhibit all of the characteristics of tidal flats during the summer months, being covered by mud nearly to the low-tide level, but in the winter the sediment in the outer to middle regions of the tidal flat comprises mainly hummocky cross-stratification (HCS) reflecting the dominant storm influence on sedimentation (Yang et al. 2005, 2006, 2008a, b). The Korean tidal flats from which the OCTF model was derived, also preserve mud at the landward end of the flats, at least locally, and in the troughs of landward translating swash bars (Yang et al. 2009). The character of preserved deposits across the Baeksu tidal flat indicates a strong storm-influence, and the evolution of storm-waves landward across the flat is manifested in an increase and then decrease in grain size (Fig. 6C). As well, there is a landward increase in the amount of bioturbation. The prevalence of HCS in the outer and middle flats (Fig. 6C) is similar to sedimentary structures seen in beach-shoreface systems (Fig. 3). However, the increase in bioturbation from the outer to the inner flats, and the decrease in grain size from the middle to the inner flats are characteristics shared with other tidal flats (Fig. 4). As such, OCTF are considered to represent a more tide-dominated expression of mixed wave-tide systems than TMS (Fig. 1A). We note that OCTFs can also be mud-dominated when downdrift of river mouths (Fan 2012; Cummings et al. 2015; Zhang et al. 2018), but we focus here on the sandy variant because of its close association with TMSs.

Despite the fact that the OCTF model was established solely on the basis of modern environments (Yang et al. 2005, 2006, 2008b), its idealized vertical, progradational succession can be reasonably derived from mapped grain-size trends, vibracore descriptions, and high-resolution seismic data (Fig. 6C). As with tidal flats, OCTFs comprise sediment exposed mainly intertidally, and hence the model includes the upper subtidal, intertidal, and supratidal zones only. Progradational expressions of OCTFs coarsen upwards in their subtidal to lower intertidal portion in a fashion similar to the upper part of progradational shorefaces and TMS. The lower and middle intertidal extent of these systems is dominated by storm-wave generated sedimentary structures. In the upper intertidal zone, OCTF exhibit a fining-upward profile reflecting the attenuation of wave energy landward across the inner flat. Subtidally, OCTFs can, theoretically, overlie deposits that are sedimentologically akin to shorefaces, TMS or delta fronts, and the middle to outer part of the flats is considered to be equivalent to the upper shoreface (Fig. 6; Dalrymple 2010). Consequently, an OCTF will probably be manifested in the rock record at the top of a storm-influenced shallow-marine succession, and be expressed as a coarsening-upward succession with interlayered bioturbated mud and sand in an overall fining-upward succession in the upper 1–3 m. It will probably be topped by rooted, muddy tidal marsh deposits if complete preservation occurs (Fig. 6C).

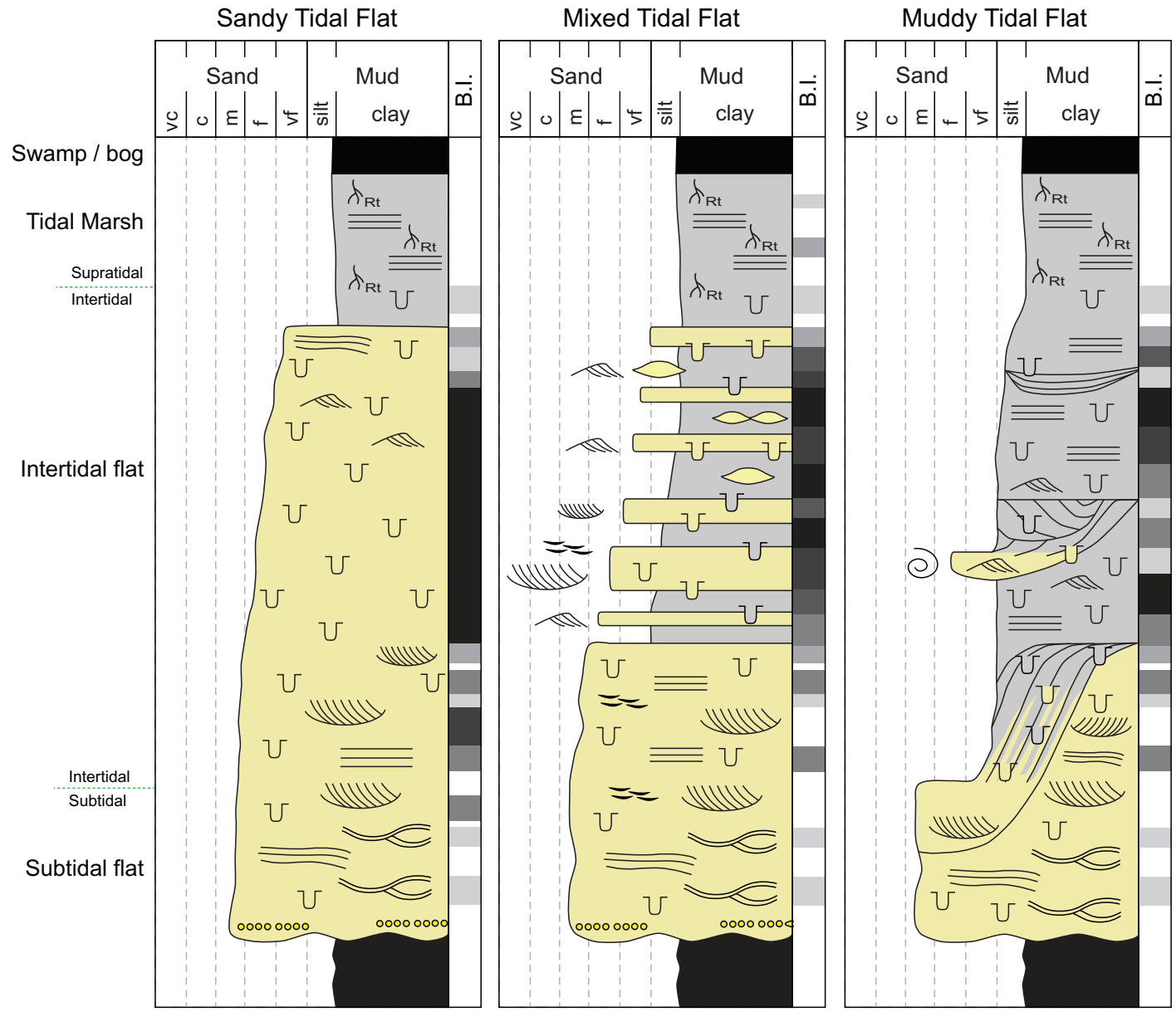

Figure 4. Conceptual models for the vertical expression of preserved, progradational tidal flats based on Boundary Bay (sand-dominated tidal flat) and Mud Bay (mud-dominated tidal flat), British Columbia, Canada. The strip logs also assume the base of the tidal-flat succession is a channel-base scour surface, although it is equally plausible that these deposits overlie and grade up from delta front or other shallow-marine strata (strip logs are adapted from Dalrymple 1992, 2010; Siddiqui et al. 2017). The vertical scale is dependent on the tidal range (in this case ~4 m for the intertidal zone). Refer to the legend in Figure 3 for definitions of acronyms, colours and symbols used in this figure.

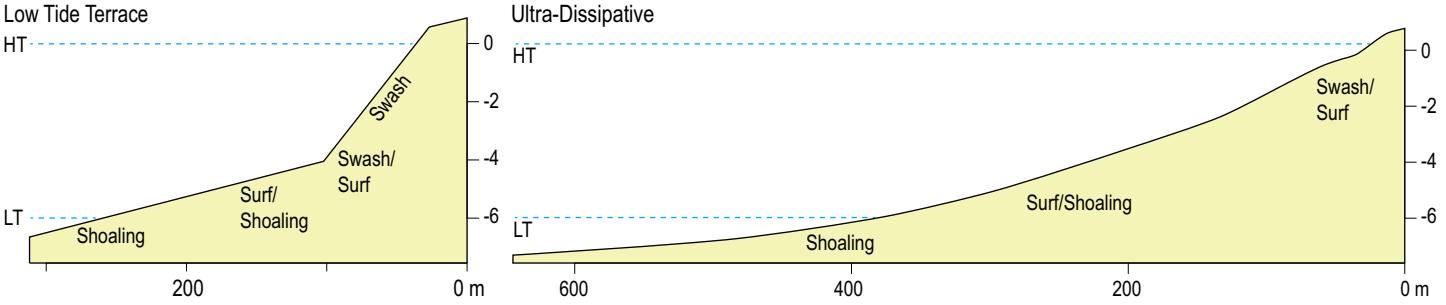

Figure 5. Two morphological profiles proposed by Masselink and Short (1993) for beach-shorefaces with strong tide influence relative to wave influence. Masselink and Short (1993) predict shorelines transition to tidal flats as tide influence increases. Acronyms: low tide (LT), high tide (HT).

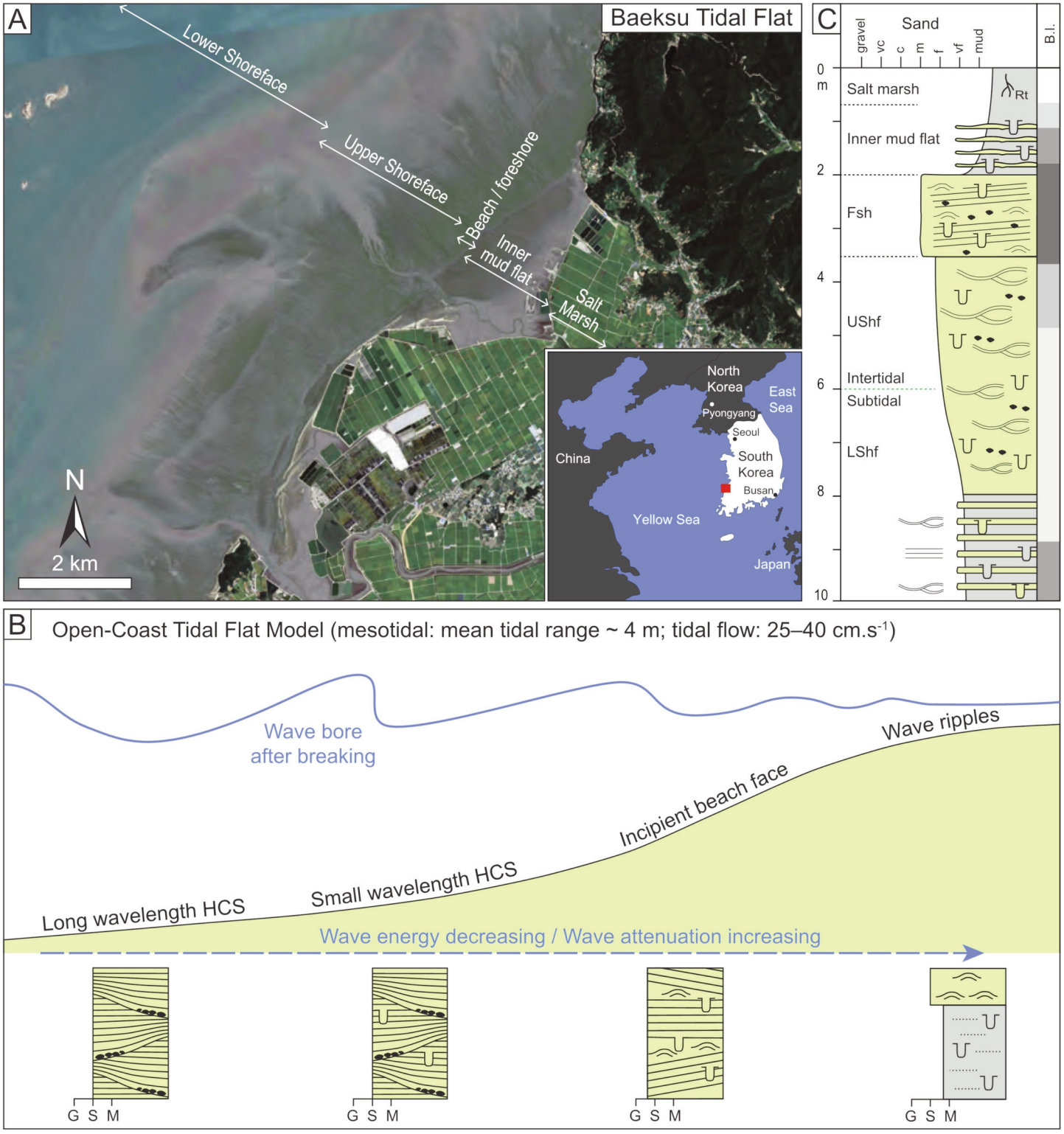

Figure 6. A) Airphoto of Baeksu tidal flat, South Korea, from which the open-coast tidal-flat model was originally derived. The approximate position of shoreface-equivalent (or tidal flat) subenvironments are demarcated by the white lines (Google Earth airphoto). B) Distribution of preserved sedimentary structures across the tidal flat (modified after Yang et al. 2005). C) Hypothetical reconstruction of a preserved vertical profile for an OCTF assuming the system is progradational. Refer to the legend in Figure 3 for definitions of acronyms, colours and symbols used in this figure.

https://doi.org/10.12789/geocanj.2021.48.171

The TMS model was developed from a beach-shoreface in the Bay of Fundy, Canada using mapped grain-size trends, boxcore and vibracore x-radiographs and descriptions, and shallow-seismic profiles (Waterside Beach, Fig. 7; Dashtgard and Gingras 2007; Dashtgard et al. 2009, 2012), and the model builds on wave-process characterization of geomorphologically similar beach-shoreface systems globally (Figs. 2D and 5; Masselink and Short 1993; Masselink and Hegge 1995). Waterside Beach experiences maximum tidal amplitudes of > 11 m and with a mean tidal range of 9 m. Wave processes dominate the system year-round with wave zones translating across the beach-shoreface with the rising and falling tide. The translation of wave zones is preserved across the beach-shoreface with different parts of the TMS being dominated by different sedimentary structures (i.e. seaward-dipping plane beds, multidirectional trough cross-stratification, HCS, etc.; Fig. 7B), but with interbedding of sedimentary structures reflecting different water depths occurring across the whole shore-normal transect (Fig. 7C). Bioturbation is reduced relative to equivalent deposits in wave-dominated beach-shorefaces, and the degree of bioturbation decreases landward, which is typical of wave-dominated beach-shorefaces. Grain size also increases in the landward direction. The onshore-offshore trends in grain size, distribution of wave-formed sedimentary structures, and degree of bioturbation in TMS is more akin to wave-dominated beach-shorefaces, and hence, TMS are considered to be a more wave-dominated expression of the spectrum of mixed wave-tide systems (Fig. 1A).

2.1 Similarities and Differences Between OCTFs and TMS

Both OCTFs and TMS as currently defined are mixed wave–tide systems where both tides and waves influence the preserved sediment character. Here we highlight the differences and similarities between the two models (Figs. 6 and 7).

1) Grain size

The small tidal prism and strong attenuation of wave energy across the gently sloping surface of OCTFs produces low-energy tidal currents and waves, which result in mud deposition across the flats, particularly during non-storm periods and in more proximal (i.e. uppermost) positions close to the high-tide level (see Fig. 8 in Yang et al. 2005). Consequently, grain size increases and then decreases in a landward direction (Fig. 6C). In contrast, TMS are persistently wave-dominated throughout their entire vertical extent, and wave processes (e.g. shoaling, breaking, swash-backwash) are partially segregated (shore-normally) under fairweather conditions (Masselink and Hegge 1995; Dashtgard et al. 2009). The dominance of wave processes across TMS is manifested in a continuous landward increase in grain size from the offshore to the surf zone, and onto the beach if the system contains gravel-sized material (Fig. 7).

2) Bedforms / sedimentary structures

The systems used to develop both the OCTF and TMS models experience numerous storms, and storm-influence is evident in preserved deposits in the form of HCS and the preservation of unbioturbated sediment. In TMS, tides are expressed in the interbedding of wave-formed sedimentary structures that result from the across-shore translation of wave zones (shoaling, surf, swash-backwash), and the accompanying tidal modulation of wave energy at any given location, with the rising and falling tide (Dashtgard et al. 2009; Vaucher et al. 2018a). For example, during high tide, swash-backwash will occur at the landward side of the beach while the lower intertidal zone will be subjected to shoaling waves and the offshore will be dominated by offshore currents (probably tidal currents). At low tide, most of the TMS is subaerially exposed: the lower intertidal zone experiences swash-backwash, and the offshore experiences shoaling waves. The preserved character of the TMS beach-shoreface is strongly influenced by storm-wave activity and the translation of wave zones during storms. In consequence, storm-derived bedforms (e.g. plane bed, hummocks and swales, 3D wave ripples, dunes) and their preserved sedimentary structures (e.g. planar lamination, HCS/SCS, trough cross stratification) in TMS are distributed across the entire offshore-to-onshore profile as a result of the rising and falling tide.

Wave-zone translation also occurs across OCTFs (as with all intertidal zones), although the distribution of sedimentary structures differs. First, the low depositional slope and attenuation of wave energy across the flats results in a landward decrease in the scale of HCS and an increase in the preservation potential of parallel-laminated and bioturbated mud in the inner to middle flats (Yang et al. 2005, 2006, 2008a,b). Second, OCTFs like Baeksu do not exhibit trough cross-stratification, and this reflects 1) the dominant sand grain size (very fine- to fine-grained sand), 2) the dominance of shoaling wave-processes during major storms and at high tide, and 3) a general absence of breaking waves and strong wave-forced currents across the flats. Third, due to the fact that wave size above shallowly submerged tidal flats is mainly a function of water depth, wave energy at any point on the tidal flat will change rapidly over each tidal cycle (namely tidal modulation of wave energy). Such depositional processes are attributed with forming two unique sedimentary deposits: wave bundles (Yang et al. 2008a) and tidally modulated storm deposits (Vaucher et al. 2017; Yang and Chang 2018; Sleveland et al. 2020) as a result of the interaction of waves and reversing tidal currents over a single tidal cycle. Tidally modulated storm deposits (Vaucher et al. 2017) and wave bundles also form in TMS. Note that descriptions of OCTFs are restricted to the intertidal zone, which is mainly equivalent to the upper shoreface and foreshore/beach. The offshore- to lower-shoreface expression of OCTFs remains largely undocumented.

3) Ichnology

In OCTFs, tidal currents operate throughout the year and supply food and oxygen to support large communities of infauna resulting in significant bioturbation in the flats (e.g. Yang et al. 2009). Yet wave reworking of the flats during storms results in high substrate mobility such that preservation of traces is low relative to most classic and sheltered tidal flats (e.g. Reineck

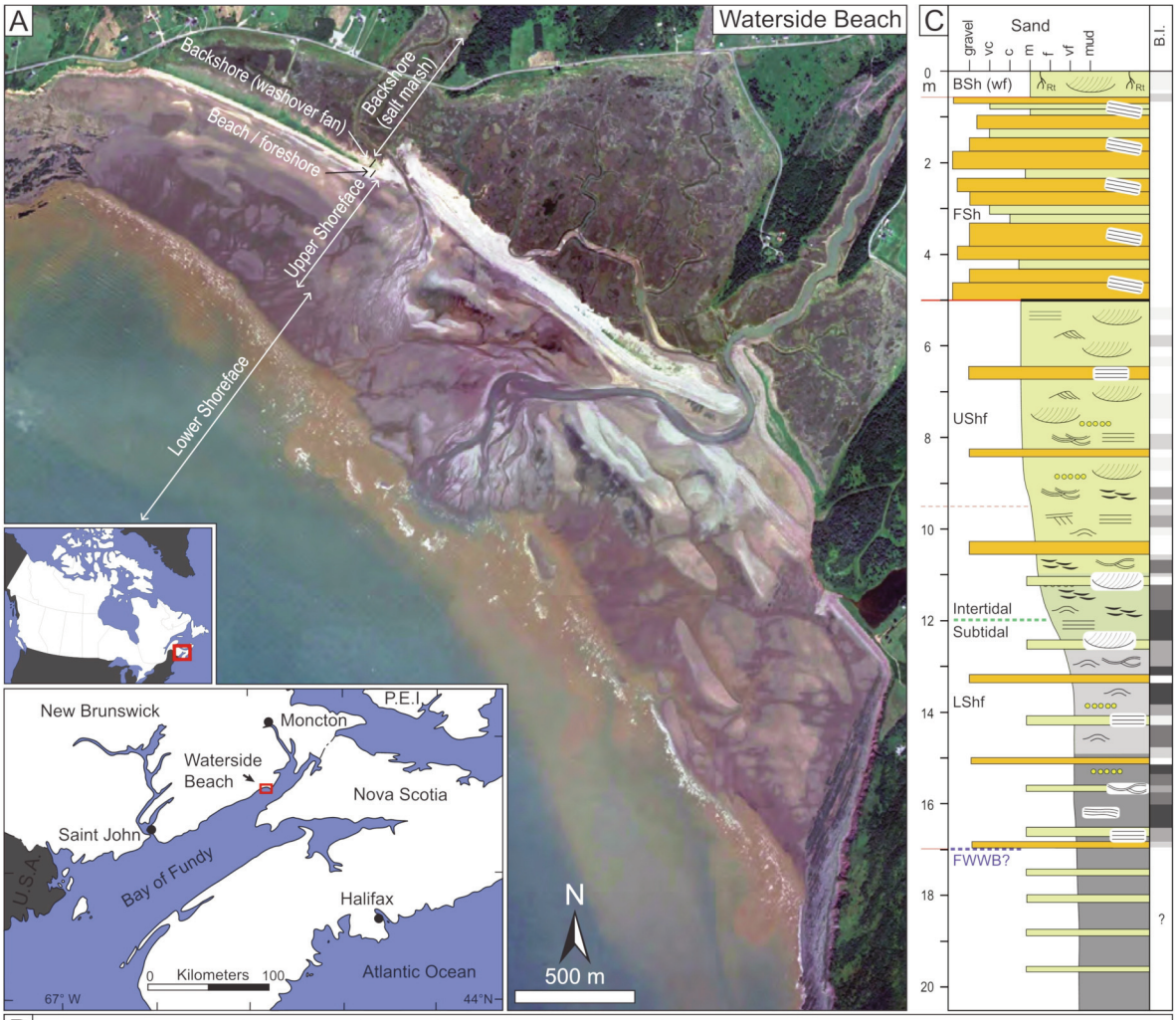

Figure 7. A) Airphoto of Waterside Beach, Bay of Fundy coast, New Brunswick, Canada, from which the tidally modulated shoreface model was derived. The approximate position of shoreface subenvironments are demarcated by the white and black lines (Google Earth airphoto). B) Distribution of preserved sedimentary structures and ichnology across the beach (modified after Dashtgard et al. 2009). C) Hypothetical reconstruction of a preserved vertical profile for a TMS assuming the system is progradational (modified after Dashtgard et al. 2012). Refer to the legend in Figure 3 for definitions of acronyms, colours and symbols used in this figure. Additional acronym: washover fan (wf).

https://doi.org/10.12789/geocanj.2021.48.171

1967; Gingras et al. 1999; Dashtgard 2011b; Dashtgard and Gingras 2012; Wang et al. 2019). TMS also show reduced bioturbation relative to microtidal beach-shorefaces due to regular subaerial exposure, high substrate mobility (arising from both the translation of wave zones during tidal cycles and tidal currents), and precipitation during exposure of the intertidal portion. The decrease in bioturbation is most pronounced in the lower shoreface (permanently subtidal to lower intertidal zone; Fig. 7; Dashtgard et al. 2009, 2012).

Both the OCTF and TMS models have existed for more than 10 years, and equivalent strata have been described from the rock record. In the next section we summarize rock record examples as they offer insights into the preserved character of tidal shorefaces that enable us to refine the tidal shoreface models described above.

3. ROCK RECORD EXPRESSIONS OF TIDAL SHOREFACES

Table 1 summarizes the published literature dealing with geological units interpreted as tidal shorefaces, either OCTF or TMS. Below we present the main recognition criteria (Table 1) used to interpret sedimentary successions as OCTF or TMS, and we provide a summary of the most frequently used sedimentary signatures.

Tidal shorefaces interpreted from the rock record (Table 1) have been identified either by recognizing the interbedding of clear tidal and wave/storm signatures in the deposits (Basilici et al. 2012; Wei et al. 2016; Bádenas et al. 2018; Kalifi et al. 2020; Sleveland et al. 2020) and/or by documenting tidal modulation of wave processes (Smosna and Bruner 2016; Vaucher et al. 2017, 2018a, 2020; MacNaughton et al. 2019; Angus et al. 2020). Tidal signatures used in these studies include tidal bundles, herringbone structures, lenticular, wavy, and flaser bedding, and mud drapes (Fig. 8A). Wave/storm processes were interpreted from low-angle to planar lamination, wave and combined-flow ripples, and HCS/SCS (Fig. 8A). Tidal modulation of wave processes was interpreted from the interbedding of oscillatory-generated structures (i.e. HCS/SCS, wave- and combined-flow ripples) of different wavelengths and within the same event bed, and in some cases, with low-angle to planar stratification (Yang et al. 2008b). This interbedding is interpreted as reflecting depth-dependent variation in storm-wave processes that resulted from the across-shore shift of wave zones as water depths vary through tidal cycles (Fig. 8B).

The sedimentary structures mentioned in the previous paragraph reflect direct wave or tide processes acting on the sediment at a given water depth; however, other criteria for combined wave-tide processes acting at the same time have been proposed. For example, Vaucher et al. (2018b) described the internal architecture of bedforms (3D dunes; see their Fig. 4) induced by supercritical backwash under fairweather conditions in the intertidal zone of a modern TMS. They hypothesized that the downcutting of the bottomsets of these bedforms reflects water-level changes during a tidal cycle (also suggested by Dalrymple and Rhodes 1995), which increased the impact of supercritical backwash at a given water depth in a relatively high-energy, wave-dominated intertidal zone. Similar sedimentary features were described from ancient nearshore strata in France and England (Vaucher et al. 2018b; Kalifi et al. 2020).

Determining the character of tidal shorefaces subtidally and into the offshore has not yet been done effectively from modern environments, but a few studies of tidal shoreface deposits from the rock record provide clues as to the character of the deeper-water part of these systems (Fig. 9; Vaucher et al. 2017). First, the distinction between a storm-dominated shoreface lacking a significant tidal overprint (Fig. 3) and a wave / storm-dominated tide-modulated system (Fig. 9) is not straightforward as the tidal signature is typically obliterated by storm processes in storm-dominated tidal shorefaces, such that the preserved offshore-to-shoreface succession is dominated by HCS and SCS (Fig. 9). The identification of a storm-dominated tidal shoreface relies on recognizing tidal modulation of storm-generated sedimentary structures or the preservation of tidal deposits formed during inter-storm periods (Table 1; Fig. 8B; Wei et al. 2016). Sedimentological evidence of tidal modulation of wave processes (e.g. Vaucher et al. 2017; Bádenas et al. 2018) includes: (i) sandstone beds displaying HCS passing gradationally upwards into combined-flow ripples and then back to HCS without evidence of multiple depositional events (i.e. deposition during one (or more) tidal cycles rather than stacked discrete storm beds); and, (ii) the pervasive stacking of oscillatory structures of shorter-to-longer wavelengths, and *vice versa*, reflecting the continuously changing water depth through tide cycles during a single storm; this acts to vary the size of the wave orbitals acting on the seafloor. Both of these stratal architectures can be interpreted as either stacked storm beds or tidal modulation of storm deposits, and so neither is diagnostic, especially if the high-energy parts of cycles are erosionally based. However, the repeated occurrences of one or both bed architectures through a conformable shoreface succession is more suggestive of tidal modulation than stacked storm beds since most storm-dominated (high energy) shoreface successions do not show significant bed-to-bed variability in the scale of HCS (e.g. Walker 1984; Plint and Walker 1987; Clifton 2006; Jelby et al. 2020).

4. A REFINED MODEL FOR TIDAL SHOREFACES

The TMS model extends from the offshore to the backshore (Fig. 7), while the OCTF occurs at elevations that are equivalent to the lower shoreface through to the backshore (Fig. 6); thus, the two models overlap spatially. Conceptually, the TMS model can be divided into lower (offshore to lower shoreface) and upper (upper shoreface to backshore) intervals. The middle shoreface is not a distinct zone in TMS or OCTF (Figs. 6 and 7) because the tidally induced lateral translation of wave zones across the intertidal zone blurs the boundaries between wave zones. In the upper interval, and under certain conditions, OCTFs and potentially other intertidal sedimentary environments can develop. Based on multiple published examples of OCTFs, both along modern coastlines and from the rock record, they typically overlie offshore to lower shoreface successions that are similar to the lower part of TMS successions. In consequence, we combine the two mixed wave-tide

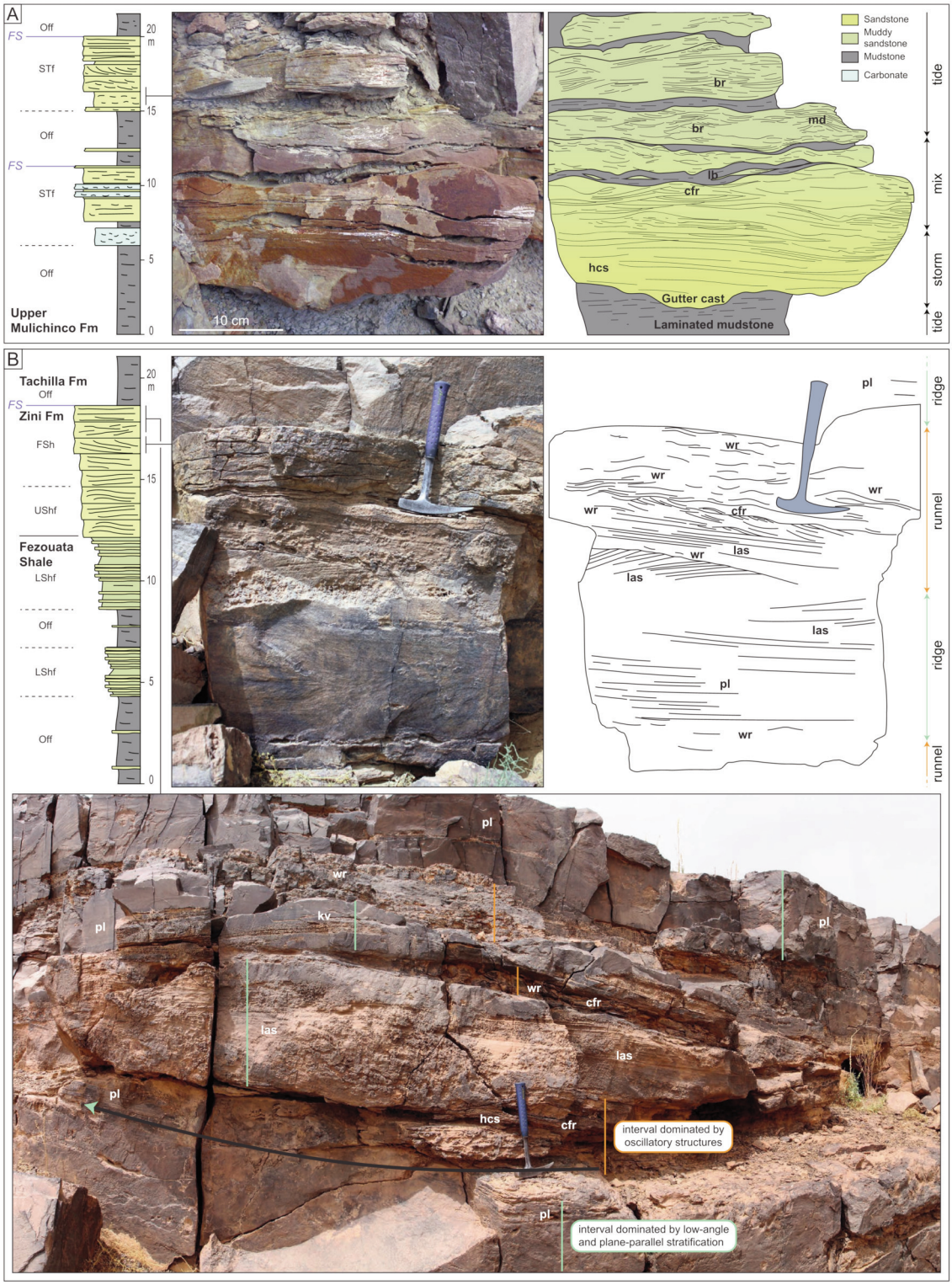

Figure 8. Examples of tidal-shoreface deposits from the rock record. A) Two parasequences that both show a shallowing-upward profile from offshore to subtidal-flat environments. The subtidal flat (STf) showcases a gradual transition from storm (sandstone) to tidal (muddy sandstone) deposits preserved in the storm-influenced (medium-energy) subtidal flat of the Upper Mulichinco Formation (Barranca Los Loros, Early Cretaceous, Argentina; modified after Sleveland et al. 2020). B) Regressive sequence that defines the Fezouata Shale and Zini Formation (Early Ordovician), which is overlain by the transgressive Tachilla Formation (Middle Ordovician), Morocco. The fine- to medium-grained sandstones from the Zini Formation are interpreted as a tidally modulated ridge-and-runnel foreshore-shoreface showcasing the repeated vertical and lateral transition from ridge to runnel in the intertidal zone (adapted from Vaucher et al. 2017, 2018a). Scale: hammer is 32 cm long. Orange and green lines refer to the colour code on Figure 9. Refer to the legend in Figure 3 for definitions of acronyms, colours and symbols used in this figure. Additional acronyms: Flooding surface (FS); bidirectional ripples (br), mud-draped ripples (md), lenticular bedding (lb), combined-flow ripples (cfr), planar lamination (pl), low-angle stratification (las), wave ripples (wr), and keystone vugs (kv).

https://doi.org/10.12789/geocanj.2021.48.171

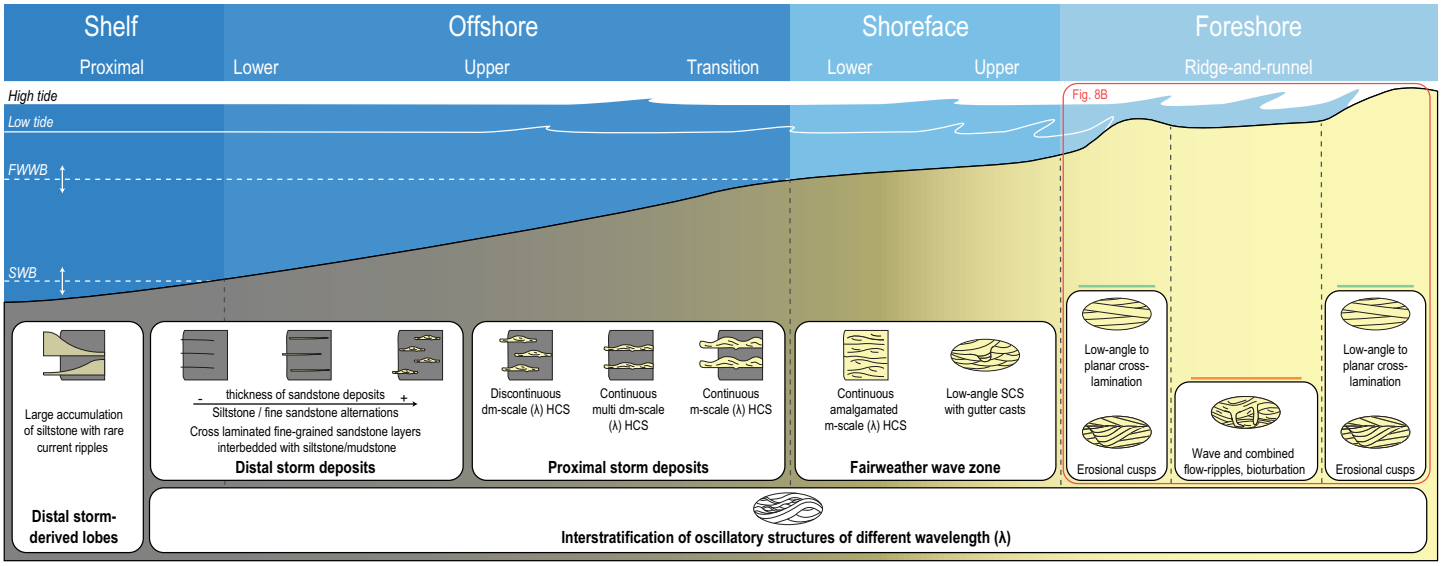

Figure 9. Facies model developed for the deposits of a wave-dominated, tide-modulated system ranging from proximal shelf to foreshore environments that occur in Fezouata Shale and the Zini Formation (Early Ordovician, Morocco; modified after Vaucher et al. 2017). Note that the overall system closely resembles a pure storm-influenced/dominated system as the succession is dominated by hummocky cross-stratification (see Figure 3). Refer to the legend in Figure 3 for definitions of acronyms, colours and symbols used in this figure.

systems into a single tidal shoreface model where TMS (as originally described) and TMS-OCTF are considered as tidal-shoreface variants along the wave-tidal continuum. We also note that TMS and OCTF are distinctive elements of mixed wave–tide systems, and so it is possible to form various combinations of OCTF and TMS with other coastal subenvironments (e.g. TMS overlain by wave-dominated upper shoreface and foreshore deposits (Fig. 7) or OCTF overlying delta-front deposits (Fan 2012; Zhang et al. 2018).

A key limitation of recognizing tidal shorefaces in the rock record is the obliteration of the tidal signature by strong storm- (high-energy) wave action. In these cases, tidal shorefaces will appear similar to storm-dominated shorefaces or storm-dominated delta fronts (compare Figs. 3 and 9). Both storm-dominated shorefaces and storm-dominated delta fronts, regardless of tidal range, are expressed as vertical successions of stacked HCS and SCS that increase in scale (thickness and wavelength) from the offshore to the lower/middle shoreface or distal delta front (Fig. 3; MacEachern et al. 2005; Hansen and MacEachern 2007; Dashtgard et al. 2012; Jelby et al. 2020). Interbedded mudstone through to muddy sandstone from the offshore to the lower/middle shoreface or distal delta front tends to be bioturbated with a decrease in the degree of bioturbation into shallower water (MacEachern and Pemberton 1992). The energy of breaking waves and turbulent wave-forced currents in the upper shoreface of storm-dominated shorefaces and proximal delta fronts of wave-dominated deltas results in preservation of trough cross-stratified sandstone (reflecting onshore and alongshore-migrating dunes and bars), and trough cross-stratified sandstones are overlain by seaward-dipping plane beds in the foreshore / lower delta plain (reflecting the vertical translation of swash-backwash; compare Figs. 3 and 7C). The cumulative vertical thickness of sedimentary strata that preserve the various wave zones in storm-dominated shorefaces and delta fronts should be greater in tidal shorefaces (or their deltaic equivalent) as a result of vertical expansion of the depth range over which the various processes operate because of the tidal range (Masselink and Hegge 1995; Dashtgard et al. 2009; Angus et al. 2020), although the facies would appear very similar. While tidal modulation of storm waves can be inferred from sedimentological evidence recorded in stacked HCS successions (see Section 3), the most reliable means to confidently distinguish a storm-dominated tidal shoreface from a storm-dominated shoreface or storm-dominated delta front is to acquire quantitative geometric data of coastal to shallow marine systems in a single parasequence. Without these data, we urge caution when interpreting a geological unit as a storm-dominated tidal shoreface.

Recognition of tidal shorefaces is easier in systems that experience low- to moderate- storm influence (Dashtgard et al. 2009, 2012). It is in such limited-energy systems that the defining characteristics of tidal shorefaces (see Sections 2.1 and 3) are most likely to be preserved, enabling their identification.

Tidal shorefaces have been described from the rock record in foreland (Basilici et al. 2012; Kalifi et al. 2020), pre-rift (Wei et al. 2016), syn-rift (Bádenas et al. 2018), post-rift (Smosna and Bruner 2016; Vaucher et al. 2017; Sleveland et al. 2020), and extensional (Angus et al. 2020; Vaucher et al. 2020) basins, as well as the margins of an epeiric sea (Table 1; MacNaughton et al. 2019). Although no general consensus exists for the type of basins in which tidal shorefaces are preserved, there is the potential for tidal shorefaces to develop more regularly on the margins of semi-enclosed basins with a tapered basin morphology that can amplify tidal currents (Dalrymple and Padman 2019). The preservation potential of tidal shorefaces is also controlled by other factors that influence preservation of shallow-marine environments including accommodation creation and sediment supply (e.g. Reading 1996). Tidal shoreface

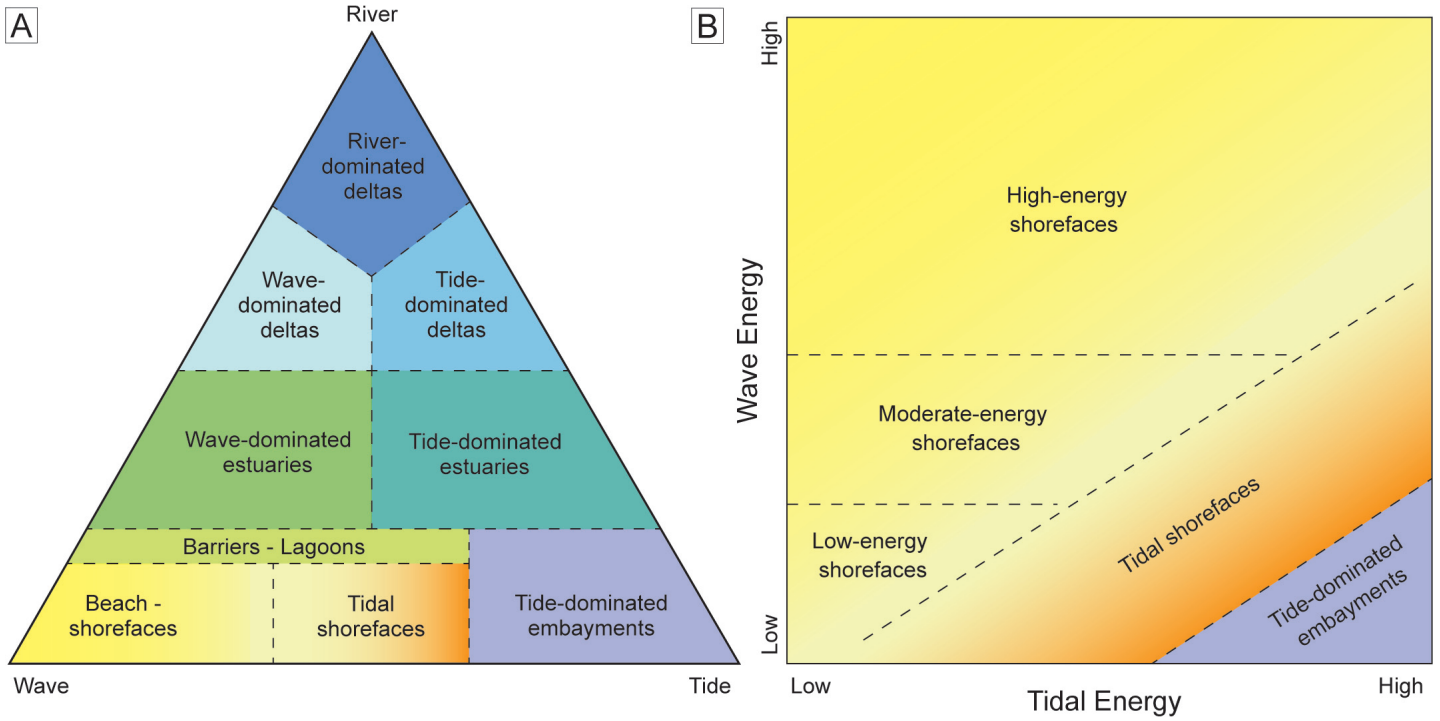

Figure 10. A) Revised classification scheme for shallow-marine and coastal depositional environments based on the relative input of energy by Rivers, Waves, and Tides. Note the merger of OCTF and TMS into a single model for tidal shorefaces, and the replacement of tidal flats at the tide-dominated apex with tidal embayments. Dashed lines indicate that all coastal environments grade into each other with changing relative energy inputs and, thus, multiple variants of these systems are possible. B) Bivariate classification of mixed wave-tide shallow-marine to coastal environments that distinguishes between low-energy waves (formerly fairweather waves), high-energy waves (formerly storm waves), and tidal processes with a range of energy levels. Note the dominance of high-energy wave processes in determining the preserved character of mixed wave-tide environments.

successions should occur more commonly in basins that experience high sedimentation and have high rates of accommodation creation (Yang et al. 2008b; Wei et al. 2016; Bádenas et al. 2018; Vaucher et al. 2018a), which suggests that tectonically active basins and river-mouth-proximal (i.e. deltaic) settings *should* favour the preservation of these systems. This hypothesis requires further investigation.

5. A REVISED TERNARY CLASSIFICATION SCHEME

In reconciling the complementary models and published examples of tidal shorefaces several issues are recognized in the widely used river-wave-tide classification scheme of coastal depositional environments and particularly along the wave-tide continuum. These issues relate to, but are not limited to, the vertical extent and position of tidal flats in coastal systems, the difference between storms and high-energy waves, and the lateral transition between various coastal systems. To address these issues, we have modified the most commonly employed coastal classification schemes (Fig. 1) with revised versions (Fig. 10), and below we explain the changes made and the reasons for them.

First, OCTFs (as with all tidal flats) occur in the intertidal zone, and hence, form only part of vertical successions representative of coastal to shallow-marine depositional environments regardless of the width of the tidal flat. Consequently, variants of tidal flats can overlie shorefaces, delta fronts, and TMS making these deposits poor candidates as a stand-alone, end-member coastal system at the tide-dominated apex of the classification scheme (Fig. 1). We have addressed this issue in the revised classification scheme of coastal environments (Fig. 10A) by replacing tidal flats with tide-dominated embayments and merging OCTFs with TMS based on the criteria discussed in Section 4. Tide-dominated embayments are commonly (but not necessarily) funnel-shaped, and the mouth of the embayment experiences strong tidal flow, and relatively little or no river input and only small waves. It is difficult to produce tide-dominated embayments with no river input or waves and so pure tide-dominated embayments are probably rare, perhaps occurring primarily in arid climate belts. Tide-dominated embayments are gradational with tide-dominated estuaries as the degree of river influence in the system increases, and tide-dominated estuaries transition to tide-dominated deltas as the volume of sediment input by rivers increases still more, leading to shoreline progradation (Fig. 10A). Two excellent examples of tide-dominated embayments include the Khor Al Adaid embayment (Rivers et al. 2020) and the Al Dakhirah lagoon (Billeaud et al. 2014) both of which are situated in Qatar.

Second, the terms "storm" and "fairweather" (cf. Fig. 1B) refer globally to the origin of waves rather than the energy of them, and consequently, do not adequately describe the wave energies experienced along all of the world's shorelines. For example, fairweather swells experienced along the west coast of Canada greatly exceed the size of storm waves experienced in Lake Erie, Canada. To address this discrepancy, we replace the fairweather wave and storm-wave apices of the fairweather wave–storm wave–tide ternary classification of mixed wave-

tide systems (Fig. 1B) with the terms low-energy waves and high-energy waves, respectively (Fig. 10B). These terms are still used in a relative sense. We also emphasize that while low-energy and high-energy are not synonymous with fairweather waves and storm waves, there is a higher probability that fairweather waves will be low-energy waves and storm waves will be high-energy waves, particularly within the same depositional system.

We also convert the fairweather wave–storm wave–tide ternary diagram (Fig. 1B) into a bivariate plot of wave energy versus tidal energy (Fig. 10B). This revised classification scheme of mixed wave-tide coastal systems remains relative where low- and high-wave energy and low- and high-tidal energy are not defined herein. This is consistent with previous publications that use relative energy inputs (e.g. Boyd et al. 1992), and with studies that have attempted to quantify tidal and wave energy, but still rely on the relative difference in energy between the two processes (Davis and Hayes 1984; Harris et al. 2002). The replacement of fairweather and storm with low-energy and high-energy, respectively, is useful because: 1) it decouples wave-energy from weather events (i.e. wave amplitudes are not dictated solely by storm intensity); 2) it accounts for the fact that wave-energy is highly variable between depositional settings; and 3) it recognizes that storm- and fairweather-waves and their products cannot be universally distinguished (c.f. Clifton 2006). The use of a bivariate plot versus a ternary diagram is also useful as it accounts for variation in tidal energy as well as wave energy (Fig. 10B). Based on this, we propose that storm-affected, storm-influenced, and storm-dominated shorefaces be renamed as low-energy, moderate-energy, and high-energy shorefaces, respectively (Figs. 3 and 10B).

The final revision of the coastal-environments classification scheme is the merger of OCTFs and TMSs into a single *tidal shoreface* model (Section 4; Fig. 10). This revision recognizes that tidal shorefaces represent mixed wave-tide systems with limited river influence (Fig. 1A) and occur in settings with low- to moderate-storm (low- to moderate-energy) wave influence. We do not expect tidal shorefaces to be recognizable if wave energy is high (Fig. 10B).

6. CONCLUSIONS

Both tidally modulated shorefaces and open-coast tidal flats demonstrate the variability in the character and architecture of mixed wave-tide coastal systems, and the models for both were developed from modern examples. Following over ten years of testing these models in modern settings and the rock record, the available evidence suggests that while OCTF and TMS are distinctive in the intertidal zone of modern shorelines, the two deposit types are likely to share comparable features in the subtidal zone. Based on this we merge the models into a single *tidal shoreface* model. The TMS model, as originally defined (Fig. 7; Dashtgard et al. 2009; Dashtgard and Gingras 2012), is considered a more wave-dominated variant of tidal shorefaces, whereas a TMS that transitions upward into a OCTF in the intertidal zone (a combined TMS-OCTF) is proposed as a more tide-dominated variant.

Tidal shorefaces are most easily identified in settings with low- to moderate-energy waves and strong tidal influence, and in settings with high rates of sediment accumulation. Recognizing tidal shorefaces in the rock record can be used as evidence of a mesotidal or greater tidal range along a paleo-coastline. Preservation of tidal shoreface deposits can also be interpreted as evidence of low to moderate storm-wave influence. In storm- (high-energy wave) dominated systems, distinguishing tidal shorefaces from microtidal (non-tidal) shorefaces is tenuous unless there is exceptional preservation of tidally generated fairweather strata and/or robust, quantified data on the geometry and character of shallow-marine geobodies. For example, a tidal shoreface in a moderate- to high-energy wave-setting should generate a succession containing thicker-than-normal intervals of trough cross-stratified beds overlain by seaward dipping plane beds at the top of the succession because of the vertical expansion of the various wave zones by tidal modulation of water levels. However, confidently identifying a storm-dominated tidal shoreface would require extensive data on the thickness of all wave-dominated beach-shorefaces along a paleo-coastline to enable identification of overthickened successions.

Tidal flats are components of a wide range of shallow-marine depositional systems including tide- and river-dominated deltas, lagoons, and tide- and wave-dominated estuaries. Many of these larger depositional environments are not tide-dominated (Fig. 1A), and therefore, tidal flats should not be situated at the tide-dominated apex of coastal classification schemes. Instead, we recommend that tide-dominated embayments occupy this position. These environments grade into tide-dominated estuaries and then tide-dominated deltas as the degree of river influence increases (Fig. 10A).

ACKNOWLEDGEMENTS

The authors thank Arve Sleveland for sharing the original file of Figure 8A. Thanks to the editor, Andrew Kerr, and reviewers Andrew Miall and Robert MacNaughton for their constructive comments on the manuscript.

REFERENCES

Ainsworth, R.B., Vakarelov, B.K., and Nanson, R.A., 2011, Dynamic spatial and temporal prediction of changes in depositional processes on clastic shorelines: Towards improved subsurface uncertainty reduction and management: American Association of Petroleum Geologists Bulletin, v. 95, p. 267–297, https://doi.org/10.1306/06301010036.

Ainsworth, R.B., Vakarelov, B.K., Lee, C., MacEachern, J.A., Montgomery, A.E., Ricci, L.P., and Dashtgard, S.E., 2015, Architecture and evolution of a regressive, tide-influenced marginal marine succession, Drumheller, Alberta, Canada: Journal of Sedimentary Research, v. 85, p. 596–625, https://doi.org/10.2110/jsr.2015.33.

Angus, L., Hampson, G.J., Palci, F., and Fraser, A.J., 2020, Characteristics and context of high-energy, tidally modulated, barred shoreface deposits: Kimmeridgian-Tithonian sandstones, Weald Basin, southern U.K. and northern France: Journal of Sedimentary Research, v. 90, p. 313–335, https://doi.org/10.2110/jsr.2020.19.

Bádenas, B., Aurell, M., and Gasca, J.M., 2018, Facies model of a mixed clastic-carbonate, wave-dominated open-coast tidal flat (Tithonian-Berriasian, north-east Spain): Sedimentology, v. 65, p. 1631–1666, https://doi.org/10.1111/sed.12441.

Basilici, G., De Luca, P.H.V., and Oliveira, E.P., 2012, A depositional model for a wave-dominated open-coast tidal flat, based on analyses of the Cambrian–Ordovician Lagarto and Palmares formations, north-eastern Brazil: Sedimentology, v. 59, p. 1613–1639, https://doi.org/10.1111/j.1365-3091.2011.01318.x.

Billeaud, I., Caline, B., Livas, B., Tessier, B., Davaud, E., Frebourg, G., Hasler, C.-A.,

Laurier, D., and Pabian-Goyheneche, C., 2014, The carbonate-evaporite lagoon of Al Dakhirah (Qatar): an example of a modern depositional model controlled by longshore transport, *in* Martini, I.P., and Wanless, H.R., *eds.,* Sedimentary Coastal Zones from High to Low Latitudes: Similarities and Differences: Geological Society, London, Special Publications, v. 388, p. 561–587, https://doi.org/10.1144/SP388.7.

Bluck, B.J., 1967, Sedimentation of beach gravels: Examples from south Wales: Journal of Sedimentary Research, v. 37, p. 128–156, https://doi.org/10.1306/74D71672-2B21-11D7-8648000102C1865D.

Boyd, R., Dalrymple, R.W., and Zaitlin, B.A., 1992, Classification of clastic coastal depositional environments: Sedimentary Geology, v. 80, p. 139–150, https://doi.org/10.1016/0037-0738(92)90037-R.

Clifton, H.E., 1969, Beach lamination: Nature and origin: Marine Geology, v. 7, p. 553–559, https://doi.org/10.1016/0025-3227(69)90023-1.

Clifton, H.E., 2006, A reexamination of facies models for clastic shorelines, *in* Posamentier, H.W., and Walker, R.G., *eds.,* Facies Models Revisited: Society for Sedimentary Geology, Special Publication, v. 84, p. 293–337, https://doi.org/10.2110/pec.06.84.0293.

Clifton, H.E., Hunter, R.E., and Phillips, R.L., 1971, Depositional structures and processes in the non-barred high-energy nearshore: Journal of Sedimentary Research, v. 41, p. 651–670, https://doi.org/10.1306/74D7231A-2B21-11D7-8648000102C1865D.

Cummings, D.I., Dalrymple, R.W., Choi, K., and Jin, J.H., 2015, Chapter 4 - Geomorphology, *in* Cummings, D.I., Dalrymple, R.W., Choi, K., and Jin, J.H., *eds.,* The Tide-Dominated Han River Delta, Korea: Geomorphology, Sedimentology, and Stratigraphic Architecture: Elsevier, p. 71–86, https://doi.org/10.1016/B978-0-12-800768-6.00004-3.

Dalrymple, R.W., 1992, Tidal depositional systems, *in* Walker, R.G., and James, N.P., *eds.,* Facies Models. Response to Sea Level Change: Geological Association of Canada, p. 195–218.

Dalrymple, R.W., 2010, Tidal depositional systems, *in* James, N.P., and Dalrymple, R.W., *eds.,* Facies Models 4: Geological Association of Canada, p. 201–231.

Dalrymple, R.W., and Choi, K.S., 2003, Sediment transport by tides, *in* Middleton, G.V., *ed.,* Encyclopedia of Sediments and Sedimentary Rocks: Kluwer Academic Publishers, p. 606–609.

Dalrymple, R.W., and Padman, L., 2019, Are tides controlled by latitude?, *in* Fraticelli, C.M., Markwick, P.J., Martinius, A.W., and Suter, J.R., *eds.,* Latitudinal Controls on Stratigraphic Models and Sedimentary Concepts: Society for Sedimentary Geology, Special Publication, v. 108, p. 29–45, https://doi.org/10.2110/sepmsp.108.03.

Dalrymple, R.W., and Rhodes, R.N., 1995, Chapter 13 Estuarine dunes and bars, *in* Perillo, G.M.E., *ed.,* Geomorphology and Sedimentology of Estuaries: Developments in Sedimentology, v. 53, p. 359–422, https://doi.org/10.1016/S0070-4571(05)80033-0.

Dashtgard, S.E., 2011a, Neoichnology of the lower delta plain: Fraser River Delta, British Columbia, Canada: Implications for the ichnology of deltas: Palaeogeography, Palaeoclimatology, Palaeoecology, v. 307, p. 98–108, https://doi.org/10.1016/j.palaeo.2011.05.001.

Dashtgard, S.E., 2011b, Linking invertebrate burrow distributions (neoichnology) to physicochemical stresses on a sandy tidal flat: Implications for the rock record: Sedimentology, v. 58, p. 1303–1325, https://doi.org/10.1111/j.1365-3091.2010.01210.x.

Dashtgard, S.E., and Gingras, M.K., 2007, Tidal controls on the morphology and sedimentology of gravel-dominated deltas and beaches: Examples from the megatidal Bay of Fundy, Canada: Journal of Sedimentary Research, v. 77, p. 1063–1077, https://doi.org/10.2110/jsr.2007.093.

Dashtgard, S.E., and Gingras, M.K., 2012, Chapter 10 - Marine invertebrate neoichnology, *in* Knaust, D., and Bromley, R.G., *eds.,* Trace Fossils as Indicators of Sedimentary Environments: Developments in Sedimentology, v. 64, p. 273–295, https://doi.org/10.1016/B978-0-444-53813-0.00010-1.

Dashtgard, S.E., Gingras, M.K., and MacEachern, J.A., 2009, Tidally modulated shorefaces: Journal of Sedimentary Research, v. 79, p. 793–807, https://doi.org/10.2110/jsr.2009.084.

Dashtgard, S.E., MacEachern, J.A., Frey, S.E., and Gingras, M.K., 2012, Tidal effects on the shoreface: Towards a conceptual framework: Sedimentary Geology, v. 279, p. 42–61, https://doi.org/10.1016/j.sedgeo.2010.09.006.

Davies, D.K., Etheridge, F.G., and Berg, R.R., 1971, Recognition of barrier environments: American Association of Petroleum Geologists Bulletin, v. 55, p. 550–565, https://doi.org/10.1306/5D25CFD3-16C1-11D7-8645000102C1865D.

Davis Jr., R.A., and Hayes, M.O., 1984, What is a wave-dominated coast?: Marine Geology, v. 60, p. 313–329, https://doi.org/10.1016/0025-3227(84)90155-5.

Fan, D., 2012, Open-coast tidal flats, *in* Davis Jr., R.A., and Dalrymple, R.W., *eds.,* Principles of Tidal Sedimentology: Springer, p. 187–229, https://doi.org/10.1007/978-94-007-0123-6_9.

Flemming, B.W., 2012, Siliciclastic back-barrier tidal flats, *in* Davis Jr., R.A., and Dalrymple, R.W., *eds.,* Principles of Tidal Sedimentology: Springer, p. 231–267, https://doi.org/10.1007/978-94-007-0123-6_10.

Frey, S.E., and Dashtgard, S.E., 2011, Sedimentology, ichnology, and hydrodynamics of strait-margin, sand and gravel beaches and shorefaces: Juan de Fuca Strait, British Columbia, Canada: Sedimentology, v. 58, p. 1326–1346, https://doi.org/10.1111/j.1365-3091.2010.01211.x.

Galloway, W.E., 1975, Process framework for describing the morphologic and stratigraphic evolution of deltaic depositional systems, *in* Broussard, M.L., *ed.,* Deltas, Models for Exploration: Houston Geological Society, p. 87–98.

Galvin Jr., C.J., 1968, Breaker type classification on three laboratory beaches: Journal of Geophysical Research, v. 73, p. 3651–3659, https://doi.org/10.1029/JB073i012p03651.

Gingras, M.K., Pemberton, S.G., Saunders, T., and Clifton, H.E., 1999, The ichnology of modern and Pleistocene brackish-water deposits at Willapa Bay, Washington: variability in estuarine settings: Palaios, v. 14, p. 352–374, https://doi.org/10.2307/3515462.

Hansen, C.D., and MacEachern, J.A., 2007, Application of the asymmetric delta model to along-strike facies variations in a mixed wave- and river-influenced delta lobe, Upper Cretaceous Basal Belly River Formation, central Alberta, *in* MacEachern, J.A., Bann, K.L., Gingras, M.K., and Pemberton, S.G, *eds.*, Applied Ichnology: Society of Sedimentary Geology, Short Course Notes, v. 52, p. 256–272, https://doi.org/10.2110/pec.07.52.0256.

Häntzschel, W., 1939, Tidal flat deposits (Wattenschlick), *in* Trask, P.D., *ed.,* Recent Marine Sediments: American Association of Petroleum Geologists, p. 195–206.

Harris, P.T., Heap, A.D., Bryce, S.M., Porter-Smith, R., Ryan, D.A., and Heggie, D.T., 2002, Classification of Australian clastic coastal depositional environments based upon a quantitative analysis of wave, tidal, and river power: Journal of Sedimentary Research, v. 72 p. 858–870, https://doi.org/10.1306/040902720858.

Hayes, M.O., 1967, Hurricanes as geological agents, south Texas coast: American Association of Petroleum Geologists Bulletin, v. 51, p. 937–942, https://doi.org/10.1306/5D25C0FF-16C1-11D7-8645000102C1865D.

Jelby, M.E., Grundvåg, S.-A., Helland-Hansen, W., Olaussen, S., and Stemmerik, L., 2020, Tempestite facies variability and storm-depositional processes across a wide ramp: Towards a polygenetic model for hummocky cross-stratification: Sedimentology, v. 67, p. 742–781, https://doi.org/10.1111/sed.12671.

Kalifi, A., Sorrel, P., Leloup, P.-H., Spina, V., Huet, B., Galy, A., Rubino, J.-L., and Pittet, B., 2020, Changes in hydrodynamic process dominance (wave, tide or river) in foreland sequences: The subalpine Miocene Molasse revisited (France): Sedimentology, v. 67, p. 2455–2501, https://doi.org/10.1111/sed.12708.

Kellerhals, P., and Murray, J.W., 1969, Tidal flats at Boundary Bay, Fraser River Delta, British Columbia: Bulletin of Canadian Petroleum Geology, v. 17, p. 67–91.

Kumar, N., and Sanders, J.E., 1976, Characteristics of shoreface storm deposits: modern and ancient examples: Journal of Sedimentary Research, v. 46, p. 145–162, https://doi.org/10.1306/212F6EDD-2B24-11D7-8648000102C1865D.

MacEachern, J.A., and Pemberton, S.G., 1992, Ichnological aspects of Cretaceous shoreface successions and shoreface variability in the Western Interior Seaway of North America, *in* Pemberton, S.G., *ed.,* Applications of Ichnology to Petroleum Exploration: A Core Workshop: Society for Sedimentary Geology, Core Workshop Notes, v. 17, p. 57–84, https://doi.org/10.2110/cor.92.01.0057.

MacEachern, J.A., Bann, K.L., Bhattacharya, J.P., and Howell Jr., C.D., 2005, Ichnology of deltas: Organism responses to the dynamic interplay of rivers, waves, storms, and tides, *in* Giosan, L., and Bhattacharya, J.P., *eds.,* River Deltas–Concepts, Models, and Examples: Society for Sedimentary Geology, Special Publication, v. 83, p. 49–85, https://doi.org/10.2110/pec.05.83.0049.

MacNaughton, R.B., Hagadorn, J.W., and Dott Jr., R.H., 2019, Cambrian wave-dominated tidal-flat deposits, central Wisconsin, USA: Sedimentology, v. 66, p. 1643–1672, https://doi.org/10.1111/sed.12546.

Masselink, G., and Hegge, B.J., 1995, Morphodynamics of meso- and macrotidal beaches: examples from central Queensland, Australia: Marine Geology, v. 129, p. 1–23, https://doi.org/10.1016/0025-3227(95)00104-2.

Masselink, G., and Short, A.D., 1993, The effect of tidal range on beach morphodynamics and morphology: a conceptual beach model: Journal of Coastal Research, v. 9, p. 785–800.

Pemberton, S.G., MacEachern, J.A., Dashtgard, S.E., Bann, K.L., Gingras, M.K., and Zonneveld, J.-P., 2012, Chapter 19 – Shorefaces, *in* Knaust, D., and Bromley, R.G., *eds.,* Trace Fossils as Indicators of Sedimentary Environments: Developments in Sedimentology, v. 64, p. 563–603, https://doi.org/10.1016/B978-0-444-53813-0.00019-8.

Plint, A.G., 2010, Wave- and storm-dominated shoreline and shallow-marine systems, *in* James, N.P., and Dalrymple, R.W., *eds.,* Facies Models 4: Geological

Association of Canada, p. 167–199.
Plint, A.G., and Walker, R.G., 1987, Cardium Formation 8. Facies and environments of the Cardium shoreline and coastal plain in the Kakwa field and adjacent areas, northwestern Alberta: Bulletin of Canadian Petroleum Geology, v. 35, p. 48–64.
Pritchard, D., and Hogg, A.J., 2003, Cross-shore sediment transport and the equilibrium morphology of mudflats under tidal currents: Journal of Geophysical Research, v. 108, 3313, https://doi.org/10.1029/2002JC001570.
Psuty, N.P., 1967, The geomorphology of beach ridges in Tabasco, Mexico: Louisiana State University Coastal Studies, v. 18, 51 p.
Reading, H.G., *ed.,* 1996, Sedimentary Environments, Processes, Facies and Stratigraphy: Blackwell Science Ltd., 704 p.
Reineck, H.-E., 1967, Layered sediments in tidal flats, beaches, and shelf bottoms of the North Sea, *in* Lauff, G.H., *ed.,* Estuaries: American Association for the Advancement of Science, p. 191–206.
Reineck, H.-E., 1975, German North Sea tidal flats, *in* Ginsburg, R.N., *ed.,* Tidal Deposits: A Casebook of Recent Examples and Fossil Counterparts: Springer-Verlag, p. 5–12, https://doi.org/10.1007/978-3-642-88494-8_1.
Rivers, J.M., Dalrymple, R.W., Yousif, R., Al-Shaikh, I., Butler, J.D., Warren, C., Skeat, S.L., and Abdel Bari, E.M.M., 2020, Mixed siliciclastic-carbonate-evaporite sedimentation in an arid eolian landscape: The Khor Al Adaid tide-dominated coastal embayment, Qatar: Sedimentary Geology, v. 408, 105730, https://doi.org/10.1016/j.sedgeo.2020.105730.
Short, A.D., 1984, Beach and nearshore facies: southeast Australia: Marine Geology, v. 60, p. 261–282, https://doi.org/10.1016/0025-3227(84)90153-1.
Short, A.D., 1991, Macro-meso tidal beach morphodynamics – an overview: Journal of Coastal Research, v. 7, p. 417–436.
Short, A.D., *ed.,* 1999, Handbook of Beach and Shoreface Morphodynamics: John Wiley and Sons, 392 p.
Siddiqui, N.A., Rahman, A.H.A., Sum, C.W., Yusoff, W.I.W., and bin Ismail, M.S., 2017, Shallow-marine sandstone reservoirs, depositional environments, stratigraphic characteristics and facies model: A review: Journal of Applied Sciences, v. 17, p. 212–237, https://doi.org/10.3923/jas.2017.212.237.
Sleveland, A.R.N., Midtkandal, I., Galland, O., and Leanza, H.A., 2020, Sedimentary architecture of storm-influenced tidal flat deposits of the Upper Mulichinco Formation, Neuquén Basin, Argentina: Frontiers in Earth Science, v. 8, 219, https://doi.org/10.3389/feart.2020.00219.
Smosna, R., and Bruner, K.R., 2016, A tide-dominated beach from the Cambro–Ordovician Cabos Formation of northwestern Spain: Journal of Sedimentary Research, v. 86, p. 1378–1398, https://doi.org/10.2110/jsr.2016.84.
Swinbanks, D.D., and Murray, J.W., 1981, Biosedimentological zonation of Boundary Bay tidal flats, Fraser River Delta, British Columbia: Sedimentology, v. 28, p. 201–237, https://doi.org/10.1111/j.1365-3091.1981.tb01677.x.
Vakarelov, B.K., Ainsworth, R.B., and MacEachern, J.A., 2012, Recognition of wave-dominated, tide-influenced shoreline systems in the rock record: Variations from a microtidal shoreline model: Sedimentary Geology, v. 279, p. 23–41, https://doi.org/10.1016/j.sedgeo.2011.03.004.
Van Straaten, L.M.J.U., 1961, Sedimentation in tidal flat areas: Alberta Society of Petroleum Geologists Journal, v. 9, p. 203–226.
Van Straaten, L.M.J.U., and Kuenen, P.H., 1957, Accumulation of fine grained sediments in the Dutch Wadden Sea: Geologie en Mijnbouw, v. 19, p. 329–354.
Van Straaten, L.M.U., and Kuenen, Ph.H., 1958, Tidal action as a cause of clay accumulation: Journal of Sedimentary Reaserch, v. 28, p. 406–413, https://doi.org/10.1306/74D70826-2B21-11D7-8648000102C1865D.
Vaucher, R., Pittet, B., Hormière, H., Martin, E.L.O., and Lefebvre, B., 2017, A wave-dominated, tide-modulated model for the Lower Ordovician of the Anti-Atlas, Morocco: Sedimentology, v. 64, p. 777–807, https://doi.org/10.1111/sed.12327.
Vaucher, R., Pittet, B., Passot, S., Grandjean, P., Humbert, T., and Allemand, P., 2018a, Bedforms in a tidally modulated ridge and runnel shoreface (Berck-Plage; North France): implications for the geological record: Bulletin de la Société Géologique de France (BSGF) - Earth Sciences Bulletin, v. 189, 5, https://doi.org/10.1051/bsgf/2018004.
Vaucher, R., Pittet, B., Humbert, T., and Ferry, S., 2018b, Large-scale bedforms induced by supercritical flows and wave-wave interference in the intertidal zone (Cap Ferret, France): Geo-Marine Letters, v. 38, p. 287–305, https://doi.org/10.1007/s00367-017-0526-2.
Vaucher, R., Vaccari, N.E., Balseiro, D., Muñoz, D.F., Dillinger, A., Waisfeld, B.G., and Buatois, L.A., 2020, Tectonic controls on late Cambrian–Early Ordovician deposition in Cordillera oriental (Northwest Argentina): International Journal of Earth Sciences, v. 109, p. 1897–1920, https://doi.org/10.1007/s00531-020-01879-9.
Walker, R.G., 1984, Shelf and shallow marine sands, *in* Walker, R.G., *ed.,* Facies Models, Second Edition: Geosciences Canada Reprint Series No. 1, Geological Association of Canada, p. 141–170.
Wang, Y.-Y., Wang, X.-Q., Hu, B., and Luo, M., 2019, Tomographic reconstructions of crab burrows from deltaic tidal flat: Contribution to palaeoecology of decapod trace fossils in coastal settings: Palaeoworld, v. 28, p. 514–524, https://doi.org/10.1016/j.palwor.2019.04.003.
Wei, X., Steel, R.J., Ravnås, R., Jiang, Z., Olariu, C., and Li, Z., 2016, Variability of tidal signals in the Brent Delta Front: New observations on the Rannoch Formation, northern North Sea: Sedimentary Geology, v. 335, p. 166–179, https://doi.org/10.1016/j.sedgeo.2016.02.012.
Weimer, R.J., Howard, J.D., and Lindsay, D.R., 1982, Tidal flats and associated tidal channels, *in* Scholle, P.A., and Spearing, D., *eds.,* Sandstone Depositional Environments: American Association of Petroleum Geologists, p. 191–245.
Yang, B.C., and Chang, T.S., 2018, Integrated sedimentological and ichnological characteristics of a wave-dominated, macrotidal coast: a case study from the intertidal shoreface of the Dongho coast, southwest Korea: Geo-Marine Letters, v. 38, p. 139–151, https://doi.org/10.1007/s00367-017-0521-7.
Yang, B.C., Dalrymple, R.W., and Chun, S.S., 2005, Sedimentation on a wave-dominated, open-coast tidal flat, south-western Korea: a summer tidal flat - winter shoreface: Sedimentology, v. 52, p. 235–252, https://doi.org/10.1111/j.1365-3091.2004.00692.x.
Yang, B.C., Dalrymple, R.W., and Chun, S.S., 2006, The significance of hummocky cross-stratification (HCS) wavelengths: evidence from an open-coast tidal flat, South Korea: Journal of Sedimentary Research, v. 76, p. 2–8, https://doi.org/10.2110/jsr.2006.01.
Yang, B.C., Gingras, M.K., Pemberton, S.G., and Dalrymple, R.W., 2008a, Wave-generated tidal bundles as an indicator of wave-dominated tidal flats: Geology, v. 36, p. 39–42, https://doi.org/10.1130/G24178A.1.
Yang, B.C., Dalrymple, R.W., Chun, S.S., Johnson, M.F., and Lee, H.J., 2008b, Tidally modulated storm sedimentation on open-coast tidal flats, southwestern coast of Korea: distinguishing tidal-flat from shoreface storm deposits, *in* Hampson, G.J., Steel, R.J., Burgess, P.B., and Dalrymple, R.W., *eds.,* Recent Advances in Models of Siliciclastic Shallow-Marine Stratigraphy: Society for Sedimentary Geology, Special Publication, v. 90, p. 161–176, https://doi.org/10.2110/pec.08.90.0161.
Yang, B.C., Dalrymple, R.W., Gingras, M.K., and Pemberton, S.G., 2009, Autogenic occurrence of *Glossifungites* Ichnofacies: Examples from wave-dominated, macrotidal flats, southwestern coast of Korea: Marine Geology, v. 260, p. 1–5, https://doi.org/10.1016/j.margeo.2009.01.008.
Zhang, X., Dalrymple, R.W., and Lin, C.M., 2018, Facies and stratigraphic architecture of the late Pleistocene to early Holocene tide-dominated paleo-Changjiang (Yangtze River) delta: Geological Society of America Bulletin, v. 130, p. 455–483, https://doi.org/10.1130/B31663.1.

Received November 2020
Accepted as revised January 2021